Investigation of Immunotoxicity of Copper-based Nanoparticles Using an *In Vitro* Inhalation Model

by

Minseok Kim

Submitted in partial fulfillment of the requirements
For the degree of Master of Science

at

Dalhousie University
Halifax, Nova Scotia
August 2020

I would like to dedicate this thesis first and foremost to God, for guiding me and strengthening me along the journey, and to my family, for everything you have done for me.

TABLE OF CONTENTS

LIST OF FIGURES

LIST OF TABLES

ABSTRACT

With a wide range of applications for nanotechnology, there is an increasing risk of nanoparticles (NPs) exposure for workers and the public. While many studies have evaluated the cytotoxicity of copper (Cu) NPs, this research investigated immunotoxicity of Cu NPs using *in vitro Streptococcus pneumoniae* (*S. pneumoniae*) infection model. Cu NPs were generated and delivered to human alveolar epithelial type II cells using an *in vitro* NP inhalation exposure system. Exposure to Cu NPs led to a dose-dependent decrease in cell viability and an increase in ROS production. Cu NPs exposed cells showed a significant increase in total number of *S. pneumoniae* adhesion. The expression of surface receptors mediating *S. pneumoniae* infection and cytokines promoting receptor expression were significantly increased in response to Cu NPs exposure. This study provides mechanistic insight into how Cu NPs enhance susceptibility to bacterial infection in human lung cells.

LIST OF ABBREVIATIONS USED

A549	Human lung alveolar type II cell line
Ag	Silver
ALI	Air-liquid interface
CFU	Colony forming unit
COPD	Chronic obstructive pulmonary disease
CPC	Condensation particle counter
Cu	Copper
DMA	Differential mobility analyzer
DMSO	Dimethyl sulfoxide
E-Cad	E-Cadherin
ECL	Enhanced luminol
EDTA	Ethylenediaminetetraacetic acid
EM	Exposure media collected from the ALI exposure
FBS	Fetal bovine serum
GSD	Geometric standard deviation
HBSS	Hank's balanced salt solution
HEPA	High-efficiency particulate air
IARC	International agency for research on cancer
ICP-MS	Inductively coupled plasma mass spectrometry
IL	Interleukin
In	Indium
INFγ	Interferon gamma
IPD	Invasive pneumococcal disease
NAC	N-acetylcysteine
NP	Nanoparticle
PAF	Platelet activating factor
PAFR	Platelet activating factor receptor
PBS	Phosphate-buffered saline
PCV	Pneumococcal conjugate vaccine
PG	Phen green SK diacetate

pIgR	polymeric Immunoglobulin receptor
PPV	Polysaccharide vaccine
psaA	Pneumococcal surface adhesin A
PVDF	Polyvinylidene difluoride
RIPA buffer	Radioimmunoprecipitation assay buffer
ROS	Reactive oxygen species
RPMI	Roswell park memorial institute
S. pneumoniae	*Streptococcus pneumoniae*
***S. pneumoniae* 4**	*Streptococcus pneumoniae* serotype 4
SDS	Spark Discharge System
SMPS	Scanning mobility particle sizer
TEER	Transepithelial electrical resistance
TGF-β2	Transforming growth factor beta 2
TiO_2	Titanium oxide
TNF-α	Tumor necrosis factor alpha
TSA	Tryptic soy agar
TSB	Tryptic soy broth
WC-Co	Tungsten carbide cobalt
Zn	Zinc
ZnO	Zinc oxide

ACKNOWLEDGEMENTS

First of all, I would like to express my deepest gratitude and appreciation to my supervisor Dr. Jong Sung Kim. Your continuous support and encouragement have guided me through my academic journey at Dalhousie. Your commitment and dedication have taught me to be a better person not only in academic field, but also in my life. Thank you for all the life lessons you have taught me in the past two years when things were going well as well as in rough moments. I would also like to thank my supervisory committee members, Dr. Zhenyu Chang and Dr. Jason LeBlanc for your guidance and expert advices throughout the degree. Thank you to my external examiner, Dr. Brendan Leung, for your time and effort put in to reading my thesis and attending the defence. Marsha Scott-Meldrum, thank you for being a huge support and responding to last minute emails.

Next, I would like to thank my lab mates at HERC lab. Erin Keltie, thank you for all the chats we had in the lab, you have been such an encouragement in the time of need. Also thank you for technical supports for ICP-MS analysis. Sydney, thank you for being a bright light to the lab. I am glad we got to know each other and pray for the best in your next chapter in life as well. Thank you to Veni, Amy, Kalli and Julia for all the talks and memories we share during lunch time and lab meetings. I would also like to give a shout out to everyone in Robertson lab. Elizabeth, thank you for teaching all your knowledge in cell culture, I am so grateful to be taught by the best in the field. Aurelio and Arul, thank you for always being there when I needed to chat about anything. Thank you for your support and friendship. All my friends in Robertson lab, Robyn N., Maddy, Sam, Gracious, Anjali, and Janet, thank you for all the fun we had in the lunchroom. Scott, I cannot express how much I appreciate your friendship in the past 9 years. From the beginning of our high school to the completion of master's degree, it has been a long and rough ride, and I cannot imagine how I could have done it without you. It will be hard to get used to not seeing you literally everyday and miss you dearly as we go on different path. I will pray for you as you move on to your next chapter.

I would like to thank my friends. Min Joon Kim, thank you for going through the same process just a year ahead of me, and giving me all the advices you have learned along the way (whether I have learned from it or not). Robyn Comeau, your expert knowledge in English has saved me on countless occasions since high school and on. Thank you for proof-reading almost every single writing I have done. Your friendship means a lot to me.

Last but not least, the biggest thanks to my family, who have supported me throughout this journey. Mom, Dad and Minji, thank you for all you have done. You have always been there for me, and I could not have come this far without you.

Chapter 1: Introduction

1.1 Metal Nanoparticles

1.1.1 Nanoparticles and its characteristics

Nanoparticle (NP) is a novel material and due to its wide range of applicable fields, it has been fluid in its definition since the time of its invention and onward, even to recent years **[1-3]**. Amongst many arguments, the most generally accepted definition of the NP is any particle with any of its dimensions less than 100 nm **[1, 4]**. When particles are engineered to nanoscale, many particles acquire novel and unique properties that are not found in a larger scale **[4, 5]**. The acquisition of novel characteristics at the nanoscale can be explained by two reasons. First, when the particles are at the nanoscale, the surface area to volume ratio increases significantly, leading to increased reactivity, so materials that are normally inert at a larger scale can be reactive at the nanoscale. Second, the quantum effect can dominate the effects of a material, leading to change in optical, electrical and magnetic behaviour of the materials **[6]**. The quantum effect, when simply put, occurs when a particle becomes small enough to reach the atomic range, altering the inherent behaviour and properties of the particle **[7]**. For example, when gold is synthesized at the nanoscale, the yellowish color changes to other colors such as red or purple. This type of characteristic is valuable as it can be applied in colorimetric biosensors **[8]**. With emergence of novel characteristics and the wide spectrum of potential applications, nanotechnology offers seemingly infinite potential to technological breakthroughs **[9]**. With increasing interest of novel technology and its potential applications, nanotechnology has been introduced into our daily lives through various fields; ranging from electronics **[10, 11]**, medicine **[12]**, sports **[13]**, cosmetics **[14]** and even to food

industry **[15]**. This is displayed through the projected global market value, where the market value of nanotechnology is expected to exceed to US$ 125 billion by the year of 2024 **[16]**.

1.1.2 Potential routes of exposure to NPs

With the increasing applications of nanotechnology, there has been on going discussion regarding exposure and potential risks associated with the products containing NPs **[6, 9, 17]**. The prominent exposure pathway of the NPs is pulmonary exposure through inhalation; however, there are other pathways that can potentially be used for exposure routes, such as ingestion and dermal exposure **[18-20]**. There are multiple exposure scenarios to metal NPs. These exposure scenarios include exposures through the usage of commercial products containing NPs, exposure to NPs through ambient air and most importantly, exposure to NPs in occupational setting **[18, 21]**.

To the general public, two of the major exposure scenarios are through the use of products containing NPs and through inhalation in ambient air. With the development of nanotechnology, there is a rapid increase in the number of products containing NPs **[19]**. There are concerns raised with regards to the hazards associated with NPs exposure through the use of these products since the early stage of development **[6]**. For example, application of remediation technology and use of fertilizers containing metal NPs can introduce metal NPs to the environment such as water and soil **[22, 23]**. Moreover, during production or transportation of metal NP incorporated in products, accidental spills may occur, resulting in metal NP entrance to the environment **[24]**. Due to their small size, NPs are easily suspended in ambient air and can stay suspended for a long duration. As a

result, there is an increased risk of being exposed to airborne NPs in ambient air to the general population **[25]**. Though the importance of particulates in ambient air has been discussed for almost a century, the presence of NPs in ambient air is a relatively novel finding, and thus in need of further studies to implement proper regulatory policies **[25]**. One of the main sources of the production of ambient NPs is the exhaust of engines. Previously, diesel engines were considered to be the main source of airborne particulate matters **[26, 27]**. However, with implementation of exhaust gas after-treatment devices, gasoline engines are also of concern for production of ambient particulate matters and NPs **[28]**. The risks associated with these exposures are relatively poorly understood, as these exposures follow repeated low-dose exposure patterns. Though these studies are of importance having close relation to the understanding of exposure risks associated with the general public, they are not well studied compared to acute exposure settings **[29]**. The general public may not be aware of their exposures to NPs, whether from the use of commercial products or through ambient air. The vulnerable population, for example, those with pre-existing pulmonary conditions such as asthma and chronic obstructive pulmonary disease (COPD), or children or elderly, may be at an increased risk of adverse health effects in response to the exposures to airborne metal NPs **[5, 30-32]**. In the absence of a routine air monitoring program to characterize NPs in ambient air, the public safety concern may persist. Without the ability to observe the elevated level of NPs in ambient air, the associated risks in NPs exposure cannot be determined and further measures to minimize exposure cannot be implemented. With these measures in place, the protection of individuals health, especially of those more sensitive to NPs exposure, can be improved.

As described, individuals can be at risk of metal NPs exposure in their daily life. However, the risk of exposure is greater in certain populations, such as workers in production of NPs containing products. Since the concentration of airborne NPs in a occupational setting is significantly greater, workers are exposed to a higher dose of NPs for longer duration **[21, 33]**. Acknowledging the risk associated with metal NPs exposure in workplaces, many metal NPs have been identified as an occupational workplace hazard by US National Institutes of Occupational Safety and Health **[33]**. However, without sufficient toxicology studies on individual metal NPs, it is difficult to determine relevant dose or concentration limits **[33]**. Therefore, to implement proper policies to protect workers from occupational exposures, there is a growing need for more toxicological studies.

Even when a relevant concentration limit has been determined, monitoring the metal NPs in ambient air can be challenging. Due to the small size of metal NPs, the traditional methods of occupational exposure assessment cannot clearly establish the risks associated with the exposure of the workplace **[34]**. The current occupational exposure regulation for airborne particulates is mainly based on mass, with exception of fibre, which is based on number **[35]**. As the uniquely small size of NPs contributes very little to the mass measured, current technology used in ambient particle monitoring cannot accurately measure the concentration of ambient metal NPs in the workplace. To overcome this limitation, recent studies suggested that the use of multi-metric approach would provide a better understanding of associated risks of NPs exposure **[36-39]**. Therefore, although the current standard monitoring regulations is in place to protect workers from larger scaled particles, it is not suitable to assess the level of NPs in the air,

and thus requires a different screening method to accurately monitor the level of airborne NPs to provide safe work environment to the workers **[38]**.

1.2 Host Responses to Metal NPs

1.2.1 Epidemiology of metal NP exposure

With many factors of NPs alone, as well as varying concentration, duration and exposure routes, the adequate risk assessment requires studies focused on specific exposure environment **[18, 40]**. As described previously, there is a high risk associated with the exposure to NPs in occupational setting, thus many studies were conducted to evaluate the hazard of metal NPs exposure. Based on numerous studies, metal NP exposures have been linked to increases in pulmonary and cardiovascular diseases **[41, 42]**.

One popular metal NP present in industrial setting is tungsten carbide cobalt (WC-Co). This WC-Co is known for its extreme hardness, stability, and resistance to wear, therefore commonly used as a spray coating on industrial tools and heavy machinery **[33]**. However, with the extended use of tools coated with WC-Co NPs, there is increased risk of exposure to airborne WC-Co NPs to the workers **[41]**. As tungsten has been classified as Group 2A carcinogen by International Agency for Research on Cancer (IARC) **[43]**, with prolonged exposure to WC-Co NPs, the exposed individuals are at higher risk of lung cancer **[44]**. WC-Co NPs specifically has been associated with occupational asthma, leading to the onset of hard metal lung disease, which is characterized by the presence of multinucleated giant cells in lung specimens **[33]**. It has also been recently established that the WC-Co NPs is capable of inducing DNA damage **[45]**. Moche et al. have proposed that the genotoxic activity of WC-Co NPs is strong

enough to be used as a positive control for *in vitro* genotoxicity assays **[45]**. Moche et al. further elucidated that the genotoxic potential by the NPs may be mediated through chromosomal damage or oxidative DNA damage **[44]**.

Titanium dioxide (TiO_2) is a naturally occurring form of titanium and has a long history of usage dating back to 1923. TiO_2 is commonly used as a whitening agent; however, its application is not limited to cosmetics, but expands to personal care products, food preparation and drug delivery **[46]**. With its large commercial applications, the exposure scenarios of the TiO_2 NPs are not limited to an occupational setting, but also includes chronic exposures through repeated use of the products by general public **[47]**. TiO_2 has been classified as a Group 2B carcinogen by the IARC in 2010; however, with the U.S. market for TiO_2 at approximately 1.31 million tons, the use of TiO_2 has not declined significantly since **[46]**. Prolonged exposure to TiO_2 NPs has been linked with damages, such as pulmonary lesions in rats **[48]** and damage to liver tissue **[49]** via increased oxidative stress, resulting in induction of cytotoxicity and genotoxicity **[46]**.

Exposures to WC-Co and TiO_2 NPs display that the exposures routes are not limited to a specific setting and that prolonged exposure to these NPs may lead to the induction of toxic response, especially in pulmonary system. The cardiovascular system is closely linked to the pulmonary system, and it has been proposed that the disruption in pulmonary homeostasis is able to cause implications in cardiovascular system as well, through multiple mechanisms **[50]**. Due to its close relation, when the exposed NPs reach the lower airway tracts, these NPs may lead to extrapulmonary responses either by direct or indirect mechanisms **[50]**. Upon the onset of pulmonary inflammation in response to

NPs exposure, secretion of cytokine on the site of inflammation can be transported to the circulation, leading to increased circulating cytokine level in the blood, which can contribute to cardiovascular pathology **[50]**. For populations with pre-existing pulmonary conditions, such as asthma or COPD, the prevalence of the disease is not correlated with cardiovascular conditions; however, as a result of such conditions, there is greater prevalence of cardiovascular risk factors **[51]**. When these individuals are exposed to metal NPs, the pre-existing conditions are exacerbated. This may result in these individuals being at higher risk for cardiovascular diseases **[50]**. In a more direct mechanism, NPs that enter the gas exchange region of lungs can be taken up by the epithelial cells and translocated to blood stream **[33, 52]**. Then, these particles can freely circulate in the blood stream, and deposit in other organs. While NPs are suspended in blood, NPs can induce recruitment of leukocytes, leading to vasculature inflammation, leading to the onset of other cardiovascular disease such as atherosclerosis **[53]**. This phenomenon is more frequently observed in metals with high solubility.

Zinc (Zn) has been used worldwide with its various fields of application, namely semiconductor, antimicrobial products, and personal care products. Amongst the top five most widely used metals in the world, zinc is listed as the fourth. The exposure risk to the metal, however, also increases with usage **[54]**. With high solubility, novel technology has adapted both Zn oxide (ZnO) NPs for the development of bioresorbable electronics such as wearable electronics **[55]**. While evidences suggest significant amount of ZnO can be found in a water-soluble form, longer term pulmonary exposure to zinc has been linked with cardiac injury and other systemic effects **[56]**. Further studies suggested that inhalation of ZnO NPs leads to deposition of ZnO NPs in end organs such as the heart,

and cause inflammation and other adverse health issues **[57]**. *In vitro* ZnO NPs toxicity study supported their implications with cardiovascular disease by suggesting that dissolved Zn ions are taken up by the endothelial cells, and are associated with coronary artery endothelial cell dysfunction by altering transcription of certain genes **[58]**.

With the epidemiology data supported by *in vivo* and *in vitro* studies, exposure to metal NPs has been linked to many pulmonary cardiovascular studies. Metal NPs entering through inhalation is deposited throughout the airway tract, causing inflammation and other damages. These NPs have been shown to be able to induce cardiovascular injury through either direct or indirect mechanisms. These toxicology studies suggests that the toxicity induced by NPs exposure is capable of causing health implications in heathy subjects; however, it is also possible that the more severe effect of the exposure could be experienced by the population with pre-existing pulmonary or cardiovascular diseases.

1.2.2 Toxicology of metal NP exposures

To properly evaluate the exposure risks associated with metal NPs, the assessment of NPs needs to be established first. When assessing the toxicity of the inhaled particles, the lung deposition of particles have to be investigated and in determining the deposition, several factors are considered such as size, density and shape of the particles **[59]**. As pulmonary route has been characterized as the major pathway for metal NPs exposure, when considering the pulmonary exposure, the particle deposition needs to be considered as well. It has been established that the particle size is important in determining the fate of the particles in regional lung deposition **[60]**. Usmani et al. has conducted a study on the

relationship between the particle size and lung deposition. The authors have had participants inhale labeled micron-sized particles with diameters of 1.5-, 3-, and 6-micron and tracked the deposition level, distal penetration, and peripheral lung deposition. They observed that the smaller sized particles (1.5-micron) have greater lung deposition, penetrated farther in distal lungs and deposited more in peripheral regions of the lung compared to larger particles (3- and 6- micron) **[60]**. The significance of smaller particles being deposited in distal regions is that these particles are able to escape the defence mechanisms in place to prevent the particles from entering the lower airway tracts. In accordance with this study, recent studies on effect of NPs exposure have provided evidences that the smaller particles such as NPs is able to deposit in the lower airway tracts (i.e. bronchioles and alveoli), and potentially be translocated to the blood stream, and circulate to other organs such as heart and brain, posing risks for secondary exposure **[33, 53, 59]**. NPs are also known to agglomerate and form bigger particles and be cleared in upper airway tracts (i.e. nasopharyngeal region). Oftentimes, when metal NPs are engineered, many manufacturers do not wish to have NPs interact and agglomerate, but rather stay in their nano-size so their desired characteristics would be preserved. This poses significant issue with human health when inhaled, as inability to agglomerate is strongly associated with less clearance and more cellular response **[40]**. Multiple studies have proposed that the smaller sized particles induce more toxicity than larger particles as smaller sized particles can penetrate deeper into the pulmonary system, reaching the gas exchange region **[61, 62]**. A study by Park et al. proposed that 20 nm silica NPs induces increased cutaneous toxicity compared to 100 nm silica NPs **[63]**. The

evidence provided suggests that the size of a particle is an important characteristic in assessing the toxicity of the particle.

Other toxicological characteristics of NPs include shape, surface, and surface corona **[40]**. Shape of particles are important in sub-micron range, as some studies have reported that depending on the shape of metal NPs of interest, there was different toxicity induced by the same material **[64, 65]**. Forest et al. have reported that when Cerium oxides NPs were exposed to macrophages *in vitro*, the rod-like NPs showed greater level of cytotoxicity and inflammation compared to cubic and octahedral shaped NPs **[64]**. Similarly, Gorka et al. have reported that silver nano-cubes exhibit less toxicity to plants compared to quasi-spherical and rod-like NPs while maintaining its desired antibacterial effect **[65]**. Many intrinsic physiochemical properties of NPs are related to its surfaces. Modification of the surface can determine the surface area, solubility, reactivity/stability and adsorption capacity of NPs. These surface properties can also be modified over time either intentionally or unintentionally, making its properties more flexible **[40]**. Coating of NPs surfaces allows for selective delivery of NPs to the target area, this application is often used for therapeutic purposes **[66]**. Consequently, the surface of NPs dictates the interaction it has with surrounding environment, the surface corona, which in turn, changes the physical properties of NPs. Therefore, understanding the potential interaction between NPs surface and their biological environment is also an important factor in determining the toxicity of NPs **[67-69]**.

With multiple factors determining the toxicological characteristics of metal NPs, it is important to consider that the toxicology of NPs is assessed with understanding of the environment the NPs are in as well as the physiochemical properties of the NPs.

1.2.3 Cellular responses to metal NPs

Oxidative stress and inflammation have been identified as an important factor in damages in response to metal NPs exposures **[70-73]**. Inflammation is a complex biological response that is an essential component of the innate immunity. In response to damages to tissues or cells by physical or chemical injuries, or pathogens, immediate response by the body is the inflammation **[74]**. However, chronic inflammation has been linked to many conditions such as cardiovascular diseases, multiple-sclerosis, arthritis and Alzheimer disease **[75]**. Most of these conditions are associated with increased production of reactive oxygen species (ROS), leading to elevated levels of oxidative stress. ROS are chemically active oxygen containing compounds that are naturally formed in the body as a result of oxygen metabolism catalyzed by nicotinamide adenine dinucleotide phosphate (NADPH) oxidase enzymes. Since ROS are toxic when present in high concentration, the body regulates the ROS level by producing antioxidants. Antioxidants are able to defend the body from ROS by prevention of generation or repairing the damage **[76, 77]**. Therefore, a steady-state level of ROS is critical in maintaining a healthy environment. When ROS production overwhelms the antioxidant activity in one's body and begins to cause damage, this phenomenon is called oxidative stress **[78]**. Oxidative stress is a key determinant in assessing the toxicity induced by NPs, as oxidative stress is a precursor to negative effects such as inflammation, cytotoxicity and genotoxicity **[79-81]**.

As described previously, the surface properties of NPs determine the reactivity of the particles. Due to high surface area to volume ratio of NPs compared to other ambient

particulate matters, NPs poses a greater risk than larger particles when inhaled. The surface of NPs is considered to be an important factor for resulting ROS production as there are potentially multiple mechanisms that can contribute to generation of ROS when NPs enter the human body **[80]**. NPs can also be directly involved in biological mechanisms like Haber-Weiss and Fenton-type reactions, in catalysis of the generation of intracellular ROS **[82]**. Therefore, the increased oxidative stress by NPs exposure is directly related to the fate of the cells.

Mitochondria play a pivotal role in cellular processes, including energy production, cell differentiation, and apoptosis **[83]**. Mitochondrion is one of the most sensitive organelle to exogenous compounds, thus it is considered to be the major target for cytotoxic effects induced by NPs **[83]**. Evidence suggests a close relationship between mitochondria and ROS production, where increased ROS production induced by NPs could cause damage to the mitochondrial function. NPs, however, can induce damage to mitochondria endogenously as well. Once NPs are taken up by the cells, cytosolic NPs can enter mitochondria and stimulate ROS generation via structural damage, impairing electron transport chain, and depolarization of mitochondrial membranes **[80, 83]**. Also, when NPs are taken up by leukocytes, these cells recognize the NPs as foreign material and begin ROS and reactive nitrogen species production via activation of NADPH oxidase enzymes **[82]**. Upon acute oxidative stress induction, mitochondria can respond by activation of the apoptotic pathway, resulting in cell death, which has been implicated as a major mechanism of cell death caused by NPs **[80]**. Based on evidences, mitochondrion is considered to be one of the major cellular compartments that is more

vulnerable to the NPs induced oxidative stress, and responsible for cytotoxicity induced by NPs exposure.

NPs exposure has been linked with genotoxicity as well. This damage is proposed to be linked to the shape of the NPs. There are two mechanisms proposed to be involved in NPs-induced DNA damage. Firstly, increased ROS and oxidative stress may cause oxidative damage to the DNA **[84]**. As oxidative stress increases, there is higher levels of free radicals in the cell, and these free radical can induce oxidative damage to the DNA **[81]**. Secondly, the NPs can directly enter nucleus through nucleopores and directly interact with DNA, resulting in destruction of the DNA double helix, and deformation of nucleotides **[85]**. While shape is important for entering the nucleus, it is also important in determining the severity of genotoxic effect. Compared to spherical nanoparticles, carbon nanotubes were able to induce significantly more DNA. Therefore, evidence suggests that the shape of NPs is critical in determining the level of DNA damage **[81]**. Therefore, NPs exposure leads to genotoxicity via induction of oxidative stress and direct interaction with the DNA strand.

There have been publications suggesting a potential relationship between NPs exposure leading to increased bacterial infections. Xu et al. had conducted a study on TiO_2 NPs which is commonly applied for its anti-bacterial capacity in combination with UV light. In the absence of the UV light, TiO_2 was shown to be toxic to eukaryotic cells, but not to bacteria **[86]**. When cells were exposed to low concentration of TiO_2, the infection by *Staphylococcus aureus* was increased by 350% compared to the healthy group **[86]**. The authors suggest that the increase in bacterial infection may be due to increased cell death, decreased activity of macrophages and direct interaction between

bacteria and TiO_2 NPs, which mediated uptake of bacteria **[86]**. Discussions regarding pulmonary exposure to ambient particulates increasing vulnerability to bacterial infection has been ongoing for a long time. Based on several epidemiology studies, when workers are exposed to welding fumes in occupational setting, they are at higher risk for respiratory illness, including pulmonary infection such as pneumonia **[87-89]**. Welding fume has been characterized to understand the potential risk associated with the exposure. The composition of the welding fume consisted of toxic gases and metal NPs **[90]**. Recent studies conducted by Suri et al. have proposed that the exposure to welding fumes increases susceptibility of the welders to infection by *Streptococcus pneumoniae* (*S. pneumoniae)* **[91]**. Therefore, studying the relationship between metal NPs exposure and *S. pneumoniae* infection can bring valuable insight into the toxicological mechanism in response to occupational exposures to welding fumes.

1.3 *Streptococcus pneumoniae*

1.3.1 *S. pneumoniae* infection and virulence factors

S. pneumoniae is a Gram-positive bacterium included in human pulmonary commensal flora. This bacteria can colonize on the mucosa surface of the airways asymptomatically **[92, 93]**. *S. pneumoniae* infection is known to be a cause of pneumonia, one of the most common causes of death in industrialized countries with the mortality rate of up to 50% **[94, 95]**. *S. pneumoniae* is an opportunistic pathogen, where normally it can colonize on human pulmonary tract as part of commensal flora and not cause any symptoms; however, when environment changes, it can become pathogenic. Spread of pathogenic *S. pneumoniae* to airway tracts can induce otitis media and pneumonia, while spread to

other sites like circulation or cerebrospinal fluid results in onset of sepsis or meningitis; these diseases are commonly termed invasive pneumococcal disease (IPD) **[89, 93, 96, 97]**. While the underlying mechanism behind the conversion of commensal state of *S. pneumoniae* to pathogenic state is not well studied, it is hypothesized that the pathogenicity of *S. pneumoniae* is determined by the nature of the strain, whether strain is inherently virulent, or the co-infection with other microbes **[96, 97]**.

In order for *S. pneumoniae* to initiate infection, it must first adhere to the host cells or environment surround the cells **[97-100]**. Commonly, infection of bacteria follows a two-step process. First, a weak and reversible interaction occurs between host and bacteria, which is followed by firm irreversible interaction which involves specific surface molecules **[101]**. Therefore, understanding the host-pathogen interaction of *S. pneumoniae* is important to prevent disease initiation and development.

There is an array of virulence factors for *S. pneumoniae* to facilitate the adhesion and invasion of the host **[102]**. Polysaccharide capsule formation, as well as biofilm formation, is critical in evading the host immune system such as complement-mediated phagocytosis and other direct killing mechanisms **[103]**. Certain serotypes of *S. pneumoniae* are known to be capable of expressing pilus. There are two types of pilus formation: one is responsible for the stimulation of proinflammatory cytokine production, and the other for adherence to epithelial cells **[102]**. Surface proteins are important virulence factors as well. One of the most studied proteins in regard to *S. pneumoniae* virulence factor is the toxin pneumolysin. It belongs to the family of pore-forming toxins. This toxin is able to bind to host membrane cholesterol and forms large pores on the host membrane, and is also known to activate macrophage and induce apoptosis **[104]**. One of

the most important steps in bacteria adhesion involves interaction between bacteria ligand and the host receptor **[98, 101, 105]**, where a firm, irreversible link is formed. As surface proteins can be recognized and further bind to the host receptor, the surface protein's interaction with the host receptor is critical in bacteria adhesion and invasion. There are well-characterized host receptors, one of them is platelet activating factor receptor (PAFR). PAFR is a G-protein coupled receptor that shows high affinity to platelet activating factors (PAF) **[106]**. Though it is an important receptor for the innate immune system **[106]**, its interaction with pneumococcal adhesin phosphocholine in facilitating adhesion and translocation of *S. pneumoniae* has been identified by Cundell et al. in 1995 **[107]**. Further study has discovered that the expression of PAFR is altered in response to exposure to cigarette smoke. *In vivo* study suggested that when mice were exposed to cigarette smoke, transcript level of PAFR was increased in their lungs, leading to increased adhesion by *S. pneumoniae* **[108]**. Other *in vitro* studies have also suggested that the co-culture of A549 cells with urban particulate matter and welding fume has increased the expression level of PAFR and *S. pneumoniae* adhesion **[91, 109]**.

Amongst the virulence factors listed above, the polysaccharide capsule formation is commonly considered to be the major virulence factors for *S. pneumoniae.* There are 92 pneumococcal serotypes known to date, and each one produces a unique polysaccharide capsules to protect itself from the host immune system **[110]**. The relationship between the degree encapsulation and virulence of *S. pneumoniae* serotype has been known for a long time **[111]**. Recent study by Weinberger et al. conducted a meta-analysis on risk associated with *S. pneumoniae* infectious disease across 92 known serotypes **[110]**. It was suggested that the IPD outcome was associated with serotype

properties, where certain serotypes exhibited lower risk and others higher risk that reference serotype 14. Amongst higher risk serotypes were type 3, 6A, 6B, 9N and 19F, and in accordance with literatures, they were more heavily encapsulated **[110]**. This study, with evidence supported by other publications, clearly demonstrates that the capsule is a major determinant for the virulence of *S. pneumoniae* **[103, 110, 112]**.

1.3.2 Current *S. pneumoniae* treatment and preventative strategies

The most common treatment for the *S. pneumoniae* infection is the use of antibiotics containing β-lactams, namely penicillin and ampicillin **[113]**. Administration of antibiotics has been shown to be effective over the years, it was shown that the treatment with antibiotics has significantly limited the spread of *S. pneumoniae* outbreak in military setting **[114]**. Additionally, in the hospitalized population with severe cases of pneumonia, current treatment regime has shown a significant increase in patient health **[115]**. Current first-line treatment contains not only β-lactams containing antibiotics, but also other antibiotics such as erythromycin for macrolides and ciprofloxacin for quinolones. However, over the last couple decades, extended use of these antibiotics has led to the acquisition of resistance for *S. pneumoniae* and other infectious bacteria, making the antibiotic treatment less effective **[116-118]**. There are still effective treatments such as fluoroquinolones and Ceftaroline fosamil that are saved for infected patients in case the first-line treatment is ineffective **[118, 119]**. However, use of these antibiotics may lead to emergence of resistance as well, leading to an increasing need for development of novel antibiotics. Development of novel antibiotics has been slowing, with only four novel classes developed in last 40 years **[120]** Therefore, the identification

of vulnerable population to bacterial infection and implementation of preventative measure is of importance in controlling the spread of *S. pneumoniae.*

As the polysaccharide capsule of *S. pneumoniae* is the primary determinant in its virulence, the vaccines are designed to target the purified pneumococcal capsular polysaccharides or protein-polysaccharide conjugates **[121]**. There are two pneumococcal preventative vaccines available: Polysaccharide vaccine (PPV) and Pneumococcal conjugate vaccine (PCV). PPV is an older vaccine which contains purified capsular polysaccharides, and PCV is newer vaccine which includes a conjugated carrier protein to capsular polysaccharides **[122]**. Although the effectiveness of PPV23 is controversial, it is still recommended for elderly population above age of 65 and individuals at high risk for IPD **[122]**. PCV is more commonly used for children under the age of 2 and adults at increased risk for pneumococcal disease in Canada **[123]**. Since the implementation of PCV7, the prevalence of IPD caused by PCV7-serotype was observed in vaccinated children as well as adults through herd immunity **[123]**. While PCV7 was successful, the incidence of non-PCV7 serotypes such as 19A was increased through serotype replacement, when void caused by reduction of serotypes covered in vaccine is replenished by non-PCV serotypes **[121, 123, 124]**. In 2009, PCV13 was licenced which included serotype 1, 3, 5, 6A, 7F, and 19A in addition to the 7 serotypes covered by PCV7. PCV13 has been used in Canada since 2011 and based on evidence taken from 2010 to 2015, PCV13 has been effective in reducing incidence of pneumococcal diseases by PCV13-serotypes, except for serotype 3 **[123]**. Since the implementation of the vaccine program, through direct vaccination and herd immunity, the morbidity and mortality of diseases by *S. pneumoniae* has decreased.

1.3.3 *S. pneumoniae* Epidemiology

Even with antibiotic treatment and vaccines available, the annual world wide morbidity in children under five years of age is approximately one million cases, and mortality approximately 200,000 cases **[93]**. It has also been estimated that amongst all deaths in children under five, approximately 30% of it has been attributed to pneumococcal infections **[125]**. Another high-risk group is the elderly population. The elderly population is more susceptible to acquisition of pneumococcal diseases, and when acquired, their mortality rate is high **[126-128]**. This can be attributed to the fact that this population presents comorbid conditions such as viral infection, chronic heart disease, chronic pulmonary disease, and diabetes **[129]**. Apart from the young and the elderly population, and the population with pre-existing conditions, workers in occupational exposure are at higher risk associated with pneumonia. Evidence suggests that individuals exposed to metal fumes, primarily welders, are at high risk for *S. pneumoniae* infection **[130, 131]**. Based on study by Wong et al., the prevalence of *S. pneumoniae* serotype 4 (*S. pneumoniae* 4) and 8 were higher in welders compared to the general population **[132]**. More recently Ewing et al. has conducted research on *S. pneumoniae* outbreak in UK, where out of four confirmed cases, three cases were caused by serotype 4 and another one by serotype 3 **[130]**. Although *S. pneumoniae 4* is not the only serotype present in outbreaks related to welder populations, based on observation and case studies, it is highly prevalent serotype. Based on the evidence provided, welders can be considered as a high-risk population for *S. pneumoniae* infection; however, under current

regime of pneumococcal vaccination program, welders are not included in the list to receive the vaccine **[133]**.

1.4 *In Vitro* Toxicology Testing Models for NP Toxicity Assessment

An *in vivo* testing method is of significant value in assessing toxicity of a material, and has been the standard method for toxic hazard assessments **[134]**. It is able to assess complex biological interactions, such as cell-to-cell and cell-to-matrix interactions, hormonal effects and, interplay of diverse cell types **[135]**. A couple drawbacks of *in vivo* toxicity study is that it is expensive, time-consuming and involves ethical issues. *In vivo* studies must follow the three Rs (Replace, Reduce and Refine), guiding principles that supports humane and ethical use of the animals **[134]**. Due to these limitations, an *in vitro* study has been favored by researchers working with nanomaterials. *In vitro* toxicology studies offer a lower cost, more convenient experimental setup, and reproducibility when compared to *in vivo* studies. Furthermore, it is not limited to ethical boundaries **[135]**. An *in vitro* study, however, is not able to replace *in vivo* study completely due to the complexity *in vivo* studies offer. There are studies suggesting that the findings from *in vitro* studies do not reflect the actual effects of NPs observed in *in vivo* settings **[135, 136]**. Therefore, it is recommended that *in vitro* studies are used in conjunction with *in vivo* studies when assessing NPs toxicity **[137]**.

In vitro studies allow for rapid and effective testing of biological endpoints, such as cell viability, genotoxicity, gene expression analysis, microscopic evaluation and mechanistic assays using specific established cell lines or primary cells in the absence of secondary effects **[137, 138]**. The selected cell line can mimic the tissue of interest from *in vivo* study, and can be selected from epithelial, endothelial, phagocytic, hepatic, blood

cell and various cancer cell line **[138]**. There is a growing number of published works assessing *in vitro* cytotoxicity of NPs using different cell lines **[137]**. With an increasing number of novel NPs development and products containing NPs in the market, there are physical limitations in terms of output rate of *in vivo* toxicology test alone. Therefore, there is a need to establish highly predictive and rapid assessment method **[139]**. As *in vitro* toxicity testing can be used for identification of potential toxicity of NPs, it is suitable to be used for high-throughput screening for NPs **[137, 140]**.

Submerged exposure is considered to be the gold standard in *in vitro* toxicology studies. With NPs of interest suspended in culture media at desired concentration, cells are easily exposed to NPs under controlled setting. However, due to unique high reactivity of NPs, and its physiochemical properties described above, the submerged exposure possess several limitations when used for testing of toxicity of NPs. For example, there have been papers proposing the limitations of using submerged exposure for copper (Cu) NPs. Adam et al. has proposed that when using submerged exposure, most Cu NPs aggregate in the medium and only a small portion is dissolved in the medium **[141]**. As described previously, the size and surface properties of NPs is crucial in determining the functionalities of NPs, this presents a great limitation in accurately assessing the toxicity of the NPs with inconsistency in exposure concentration as well as physiochemical properties.

To overcome limitations presented by the conventional submerged *in vitro* system, a better culture method has been developed at an air-liquid interface (ALI). Various types of the ALI exposure system has been developed to study the inhalation effects of exhaust emissions, nanomedicines, cigarette smoke and occupational exposure

to NPs **[142]**. Advantages of the ALI exposure system is that it allows for delivery of NPs directly to the cells on the interface where apical membrane of the cells is exposed to air and basolateral membrane is in contact with culture medium. NPs are delivered through the air and directly to cells, providing a more accurate presentation of pulmonary model for inhalation exposure as well as controlled and efficient delivery of NPs compared to traditional submerged exposure system **[142, 143]**. Another advantage of using the ALI *in vitro* exposure system is that when cells are cultured in the ALI system, they undergo changes in surface properties to adjust to the exposure environment **[144]**. A study by Ohlinger et al. suggested that when alveolar type II cells (A549) are cultured in the ALI system, cells start producing surfactant and changes surface properties which are not observed in traditional submerged system **[144]**. The authors also state that this change in surface properties and production of surfactant would also occur in *in vivo* setting, suggesting close resemblance between the ALI system and *in vivo* setting **[144]**. Therefore, the use of the ALI system can overcome the limitations presented by traditional submerged *in vitro* exposure system, and more accurately predict the effects of inhalation exposure to metal NPs.

1.5 Hypothesis and Objectives

Based on previous studies in the lab, the toxicity of Cu NPs was evaluated using *in vitro* submerged exposure and *in vivo* study **[145]**. Through *in vitro* submerged exposure, mechanistic insight to cytotoxic effect of Cu NPs had been elucidated. Exposure to Cu NPs induced ROS generation, which led to increased oxidative stress and inflammation. The oxidative stress resulted in cell death through either apoptosis or necrosis. The link

between Cu NPs exposure and cellular damage had been outlined; however, the study would be strengthened with the use of the ALI exposure system instead of traditional submerged exposure system. Moreover, it was observed that exposure to Cu NPs significantly increased bacterial infection with both *in vitro* submerged exposure study and *in vivo* animal study **[145]**. These studies, however, did not provide any mechanism link between the Cu NPs exposure and enhanced bacterial infection. Therefore, the current project aims to investigate the mechanisms of cytotoxicity induced by Cu NPs and provide the missing link between Cu NPs exposure and enhanced bacterial infection with the use of *in vitro* ALI exposure system.

The main objective of the study is to elucidate the mechanism behind the immunotoxicity of airborne Cu NPs exposure on enhanced bacterial infection using the *in vitro* NPs exposure model. The immunotoxicity is defined as adverse effects of exposure to toxic substances on the functioning of immune system in both local and systemic level **[146]**, which is suitable description of the effects of Cu NPs being investigated in this study. The central hypothesis of the study is that the Cu NP-induced oxidative stress and inflammation promotes increased expression of surface receptors that lead to enhanced bacterial infection.

In order to test the hypothesis, three objectives were established:

Objective 1. To assess the cellular responses of inhalation exposure to Cu NPs using human lung alveolar type II cell line (A549).

The toxicity study of Cu NPs has been conducted using *in vitro* submerged exposure models; however, in order to assess the following objectives, the cytotoxic potential has to be verified using the *in vitro* ALI exposure system. In this objective, delivery of Cu NPs and cellular uptake by A549 were measured, as well as cell viability and intracellular ROS level. It is predicted that the Cu NPs delivery to A549 and cellular uptake of Cu NPs are confirmed; cell viability is decreased; and intracellular ROS level is increased in dose-dependent manner in Cu NPs exposure group.

Objective 2. To determine the levels of bacterial adhesion in response to Cu NPs exposure using a cell-bacterial infection model.

The bacteria adhesion level was measured following Cu NPs ALI exposure to determine the enhanced vulnerability of A549 cells to *S. pneumoniae* infection. It is predicted that in accordance with previous finding, A549 cells exposed to Cu NPs exhibit higher number of bacteria adhered compared to control dose-dependently.

Objective 3. To identify how airborne exposure of Cu NPs enhances bacterial infection by characterizing the role of the surface receptors in Cu NPs-exposed lung cells.

To elucidate the mechanisms of immunotoxicity induced by Cu NPs, host receptor-bacteria ligand interactions were evaluated by specifically focusing on the change in protein and gene expression of host receptors in response to Cu NPs exposure. Furthermore, cytokines and chemokines involved in receptor expression pathway was

measured as well. It is predicted that the host receptors show dose-dependent increase in both protein and gene expression, and the associated cytokines are affected in similar pattern.

Chapter 2: Materials and Methods

2.1. NPs Generation and Characterization

The NPs were generated using the Spark Discharge System (SDS). Two Cu electrodes (99.999%) were placed about 2-3 mm apart, and high voltage was applied using HV Rack System (UltraVolt, Ronkonkoma, NY, USA), generating spark between the electrodes. The generated NP aerosol were delivered through electrostatic dissipative tubing with 3.8 L/min nitrogen and then 0.95 L/min oxygen and 0.25 L/min carbon dioxide were added to NP aerosol. The size and number concentration of NP aerosols were measured by Scanning Mobility Particle Sizer (SMPS, TSI Incorporated, Shoreview, MN, USA) consisting of nano Differential Mobility Analyzer (DMA) and Condensation Particle Counter (CPC). The size distribution for monodisperse NP aerosols was continuously monitored using SMPS for optimal condition with consistent number concentration, particle size and geometric standard deviation (GSD). The size distribution for monodisperse particles are considered as a GSD of less than 1.6 **[147-150]**. Change in the distance between the electrodes resulted in alteration in voltage and current, which allowed for the achievement of optimal condition.

2.2. Cell Culture

The reagents for culturing cells such as Roswell Park Memorial Institute (RPMI) 1640 media, fetal bovine serum (FBS), penicillin/streptomycin, Gentamycin, phosphate-buffered saline (PBS) pH 7.4, trypan blue reagent, trypsin-Ethylenediaminetetraacetic acid (EDTA) (0.25%) were purchased from Thermo-Fisher (Waltham, MA, USA). N-Acetylcysteine (NAC) was purchased from Sigma-Aldrich (Brockville, ON, Canada).

Culturing devices such as vented culture flasks, multi-well plates, and 6 well transwell inserts were purchased from Corning Life Sciences (Corning, NY, USA).

A549 cells were selected for this study as inhaled NPs are likely to deposit in alveolar airspaces and on alveolar epithelial surfaces **[59]**. Alveolar epithelium lines the airways and constitutes the first line of innate defense against respiratory pathogens. Usually, this epithelial barrier restricts the accumulation of fluid and large solutes in the alveolar spaces **[151]**, but injury disrupts its barrier function, allowing access of inhaled particles to deeper layers of the mucosa. A549 cells were purchased from ATCC (Manassas, VA, USA), and cultivated in a culture media, consisted of RPMI 1640 medium, 10% FBS, 1% penicillin/streptomycin and Gentamycin under humidified atmosphere containing 5% CO_2 at 37 ºC.

2.3. NPs Exposure System

2.3.1. Air-Liquid Interface (ALI) Exposure

In preparation for NPs exposure, A549 cells were cultured to 80% confluency on tissue culture flask and were harvested using Trypsin-EDTA (0.25%). Collected cells were washed with PBS and counted by Hemocytometer with Trypan blue stains. Then they were diluted using culture media to the concentration of 200,000 cells/mL. Prior to the seeding of the cells, transwell membrane inserts were conditioned with A549 culture media by adding 2 mL of the culture media to the basal side of the membrane and incubating it for 30 minutes. This conditioning allows better attachment of the cells to the porous membrane. Then, 1 mL of the diluted solution was added to the apical side of the transwell membrane (200,000 cells/well). Cells were incubated on the transwell for 24

hours under submerged condition at 37 ºC.

16 hours prior to the exposure, culture media on the basal side was replaced with fresh media, and culture media on the apical side was removed. This was done to condition A549 cells to the environment that the exposure will be conducted under, where apical surface would be exposed to the air and basal surface in contact with culture media, as displayed in **Figure 2.3.1**.

Immediately prior to the exposure, 17.5 mL of 37 °C culture media was added to each well of exposure chamber (Vitrocell®, Waldkirch, Germany), containing 4 wells total, then the transwell inserts with A549 monolayer was transferred to the chamber in the biosafety cabinet. Once the insert containing cells was transferred to the chamber, exposure chamber containing cells was then attached to the ALI exposure system. This ALI exposure system allowed constant aerosol flow rate of 10 mL/min for each individual chamber. The aerosol was comprised of 3.80 L/min nitrogen, 0.95 L/min oxygen and 0.25 L/min carbon dioxide, and generated Cu NPs as described previously. For Cu NPs exposure, NPs were delivered to A549 cells via the ALI exposure system for either 2 or 4 hours. For air exposure as a control, high-efficiency particulate air (HEPA) filter (PALL, Port Washington, NY, USA) was attached to the system to remove Cu NPs and NP-free aerosols were delivered to the cells. Throughout the exposure, the temperature of the exposure chamber was maintained at 37 °C with water circulating through the walls using Alpha A-6 circulating water bath (Lauda-Brinkmann, Delran, NJ, USA) and particle size distribution was regularly monitored using the SMPS. The ALI exposure system used in this study is presented in **Figure 2.3.2**.

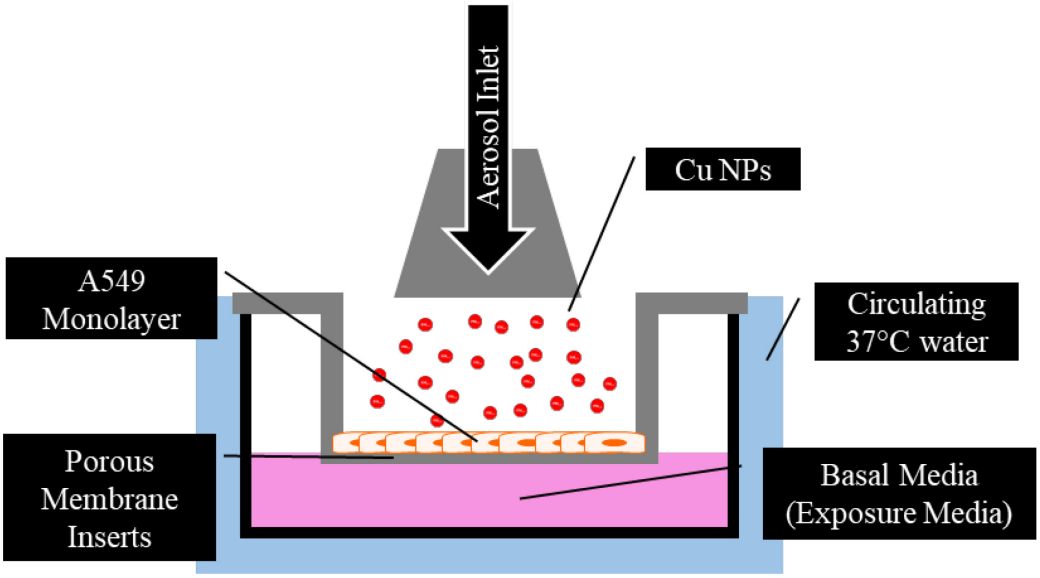

Figure 2.3.1 Schematic view of the Air-Liquid Interface (ALI) Exposure Chamber. A549 cells are seeded on porous membrane to form a monolayer. Cu NPs are delivered at flow rate of 10 mL/min to the apical membrane of the monolayer. Basal membrane is in contact with culture media

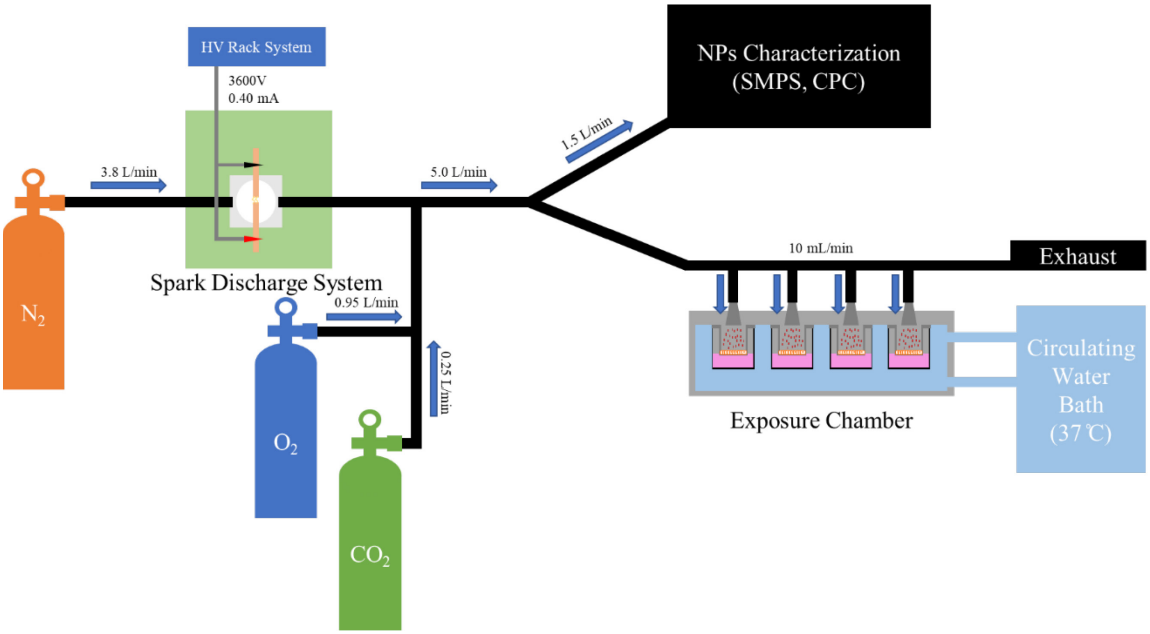

Figure 2.3.2 Schematic diagram of the ALI exposure system. 3.8 L/min nitrogen, 0.95 L/min oxygen and 0.25 L/min carbon dioxide are combined to make 5.0 L/min of ambient air condition. Cu NPs is generated through Spark Discharge System and delivered to SMPS and CPC for NPs characterization and Exposure Chamber to delivery to cells. Remaining particles and gas are disposed. Exposure Chamber is kept at 37 ºC using Circulating Water Bath.

For NAC experiment, 24 hours prior to the exposure, media was replaced with fresh culture media with NAC at the final concentration of 5 μM. Immediately prior to the exposure, NAC containing media was removed and fresh media was added for the further process.

Following the exposure, cells were washed with 1 mL of warm PBS, and inserts were replaced to 6 well plates with 2 mL fresh basal culture media for further experiments. PBS wash solution was collected and stored at -80°C freezer for future analysis. The culture medium from the exposure chamber was collected and stored at -80°C for future experiments such as submerged exposure. This media is herein referred to as Cu NPs exposure media (EM).

The use of EM for the submerged NP exposure is different than the conventional submerged NP exposure in that EM contains more than just metal NPs. As aforementioned, conventional *in vitro* submerged NP exposure involves addition of metal NPs directly to the media, resulting in potential agglomeration and change in physiochemical properties of the NPs. The EM collected from the ALI exposure contains not only the metal NPs, but also dissolved metal ions and cellular mediators released from cells following the ALI exposure.

2.3.2. Submerged NPs exposure

For the submerged NPs exposure, cells were collected and diluted to the concentration of 200,000 cells/mL as described previously. Cells were seeded to 12 well plate, by adding 1 mL of solution to each well (200,000 cells/well) and were incubated at 37 °C for 48 hours until it reaches approximately 80% confluency. Once the cells reach the

confluency, the culture media was replaced with respective EM (NP-free air exposure, 2-hour NPs exposure, 4-hour NPs exposure), and cells were incubated with the EM for 24 hours at 37 °C prior to further experiments.

2.4. Cellular Response to Cu NPs Exposure (Objective 1)

2.4.1. Cellular Cu NPs uptake

In order to confirm that Cu NPs are taken up by the cells and determine the concentration of Cu NPs delivered, the Phen Green SK, Diacetate (PG, Thermo-Fisher, Waltham, MA, USA) was used to test the intracellular di-cationic heavy metals. PG powder was dissolved in Dimethyl Sulfoxide (DMSO, VWR, Franklin, MA, USA) to the stock concentration of 2.6 mM and dissolved in culture media to the final concentration of 5 μM prior to treatment to the cells. Cells were incubated in the media containing PG for 1 hour under dark condition. The PG media was removed, and cells were washed with PBS prior to being exposed to Cu NPs. Following the exposure, cells were washed and lysed using 1% Triton X-100 diluted with PBS. The fluorescence was measured using the Synergy H1 microplate reader (BioTek, Winooski, VT, USA) with excitation 490 nm, emission 530 nm. Experiments were performed in triplicates in 24 well plate.

2.4.2. Cell viability

Cell viability was measured using MTT (Thermo-Fisher, Waltham, MA, USA). MTT dye was dissolved in Hank's Balanced Salt Solution (HBSS, Thermo-Fisher, Waltham, MA, USA) to the concentration of 5 mg/mL. This stock solution was aliquoted in 10 mL and stored in -20℃ freezer away from light.

Following the ALI exposure, the inserts were transferred to a new 6-well plate and washed with warm PBS. Stock MTT solution was thawed and diluted 1 in 10 with culture media. 1 mL of working solution of MTT dye was added to the apical side of each insert. The cells were then incubated at 37 ºC humidified air containing 5% CO_2 under dark conditions for 2 hours. Following the incubation, the MTT solution was removed, cells were gently washed with PBS and 1 mL of DMSO was added. Once all the crystals were fully dissolved, the solution in the inserts was transferred to 6-well plate for the absorbance reading. The absorbance values were read using the Synergy H1 microplate reader (BioTek, Winooski, VT, USA) at 562 nm. For submerged NP exposure, the experiments were performed in triplicates in 24 well plate, and same procedure was followed as the ALI exposure except for transfer from inserts to 6-well plates.

2.4.3. Intracellular ROS generation

Carboxy-H_2DCFDA (Thermo-Fisher, Waltham, MA, USA) was used to determine levels of intracellular ROS generation. Following the ALI NP exposure, cells were washed with PBS. A working solution of Carboxy-H_2DCFDA reconstituted in DMSO (concentration of 1 mM) was diluted in HBSS to a final concentration of 25 µM. 1 mL of final solution in HBSS was added to the apical side and incubated under dark conditions for 30 minutes (37 ºC, 5% CO_2). Following this incubation, cells were washed with PBS, and 1 mL of Triton X-100 (0.1% solution in PBS) was added to apical side, the plate was placed in a shaker for 30 mins. 100 µL of lysate was transferred to a 96-well plate. The fluorescence intensity was measured with excitation of 485 nm and emission at 530 nm using the Synergy H1 microplate reader (BioTek, Winooski, VT, USA).

2.5. Bacteria Adhesion Level in Response to Cu NPs Exposure (Objective 2)

2.5.1. *S. pneumoniae* serotype 4 culture

S. pneumoniae 4 has been generously provided by Dr. Jason LeBlanc (Infectious Diseases Lab, Halifax, NS, Canada). With the new batch of bacteria, it was necessary to validate the growth and correspond the OD600 value to specific Colony Forming Unit (CFU) in order to carry out the further experiments. OD600 value was measured using NanoDrop One Microvolume UV-Vis Spectrophotometer (Thermo-Fisher, Waltham, MA, USA).

Inoculum of *S. pneumoniae* 4 was plated on TSA II with 5% sheep blood (BD Diagnostics, San Jose, CA, USA). 24 hours later, the lawn of *S. pneumoniae* 4 was transferred to 10 mL of Tryptic Soy Broth (TSB, Sigma-Aldrich, Brockville, ON, Canada) the starting OD600 value was adjusted to 0.3 to ensure the same starting concentration for all experiments. OD600 value was measured at 0 h, 6 h, 11 h, 12 h, 13 h, 14 h, 15 h, 16 h, 18 h, and 24 h mark since the beginning of liquid culture. While obtaining OD600 values, CFU count plating was conducted every 6-hour mark. Serial dilution was performed on the liquid culture stock and each dilution was plated on TSA II blood agar plate between 10^4 to 10^8. CFU was counted the next day.

2.5.2. Bacteria adhesion assay

Two days before the infection, *S. pneumoniae* 4 was plated onto TSA II blood agar plate, then passed to a new plate 16 hours prior to the infection.

For both submerged and the ALI exposure, same procedure was followed as described in **section 2.3.1 and 2.3.2**, except for the culture media used. 16 hours prior to

the exposure, antibiotic free culture media was added to the inserts, where penicillin/streptomycin and Gentamycin were not added to the culture media as it will interfere with *S. pneumoniae* 4 infection.

Following the exposure, cells were washed with PBS, and were infected with *S. pneumoniae* 4 at the MOI of 10 for 2 hours. Following the infection, cells were washed with PBS and detached with 2 mL of Trypsin 0.25%, incubated in 37 ºC for 5 minutes. For cell lysis, 8 mL of Saponin 0.1% (Alfa Aesar, Ward Hill, MA, USA) in PBS (w/v) was added and cells were kept in 37 ºC for 10 minutes. Lysates were diluted to the factor of 100 and plated on TSA II blood agar plates. CFU count was done the next day.

To ensure the number of bacteria used for the infections was consistent across different studies, one control plate was used for each infection. *S. pneumoniae* 4 was suspended in PBS at the OD600 of 1.0, the solution was diluted at the factor of 10^7, and plated on TSA II blood agar plates. The CFU count was done the following day, and studies with CFU value 50-100 were accepted as consistent bacterial infection.

2.6. Host Receptor Expression Level (Objective 3)

2.6.1. Western Blot

For Western Blot assay, Radioimmunoprecipitation assay buffer (RIPA buffer), protease inhibitor cocktail, polyvinylidene difluoride (PVDF) membrane and enhanced luminol (ECL) Prime western blotting detection kit were purchased from Sigma-Aldrich (Brockvill, ON, Canada). Protein ladder, Lammali buffer, Bradford Assay kit were purchased from Bio-Rad (Hercules, CA, USA). E-Cadherin (E-Cad), Platelet Activating Factor Receptor, β-Tubulin unconjugated primary antibodies and HRP conjugated Goat

Anti-Rabbit secondary antibody were purchased from Abcam (Cambridge, UK).

Immediately prior to the completion of the ALI exposure, lysis buffer was prepared on ice with 1:1:8 ratio in volume of RIPA lysis buffer, protease inhibitor, ice-cold PBS accordingly. Following the ALI exposure, total cellular proteins were extracted, by adding 100 µL of lysis buffer to each insert and the plate was placed on temperature-controlled shaker at 4°C, 200 rpm for 30 minutes. Cell lysates were collected to 1.5 mL Eppendorf tubes, and centrifuged for 15 minutes at 14,000 g. Supernatant was collected and protein level was measured using Bradford Assay according to protocol provided by the manufacturer (Bio-Rad, Hercules, CA, USA). The protein samples were aliquoted to 20 µL and stored in -80℃ freezer for further experiment. On the day of Western Blot assay, the protein samples were thawed on ice, and prepared by adding 10 µL Laemmli buffer (5% 2-Mercaptoethanol) with 10 µg of protein and topped to 20 µL with type-I water. Protein samples were loaded to SDS-PAGE gel with 4% acrylamide stacking gel and 12.5% acrylamide lower gel. Protein separation was run at 70 V for 10 minutes, then 140 V for 2 hours. Protein transfer to PVDF membrane was run at 350 mA for 45 minutes. The chamber was placed in ice-water bucket for the transfer process.

Membranes were blocked with 5% skim-milk in TBS-T and washed three times with TBS-T prior to visualization with corresponding primary antibodies. Membrane was incubated with primary antibody on a shaker overnight in cold room. Primary antibodies were added at 1/1000 for PAFR and β-Tubulin, and 1/10000 for E-Cad in concentration as recommended by manufacturer. For secondary antibody, membranes were washed 3 times with TBS-T for 5 minutes each, and secondary antibody was added at 1/10000 concentration and was left on shaker for 1 hour in room temperature.

Protein bands were visualized using ECL Prime western blotting detection kit and imaged with Bio-Rad ChemiDoc™ Touch (Bio-Rad, Hercules, CA, USA). Image was analyzed with Image Lab 6.1 Software provided by Bio-Rad.

2.6.2. RT-qPCR

For RT-qPCR, Aurum Total RNA Mini Kit, iScript cDNA synthesis kit, SsoFast EvaGreen Supermix kit, green shell/white well PCR plates, Adhesive Seals were purchased from Bio-Rad (Hercules, CA, USA). Primers for reference genes and genes of interest were purchased from Thermo-Fisher (Waltham, MA, USA).

Following NPs and NP-free ALI exposures, RNA was extracted with an Aurum Total RNA Mini Kit from A549 cells. The spin protocols were performed according to the manufacturer's instructions. RNA quantification, integrity and purity check were performed using an Epoch microplate spectrophotometer (BioTek Instruments, Winooski, VT, USA). Reverse transcription was carried out with the iScript cDNA synthesis kit using 1000 ng of template RNA for each sample. For the reverse transcription, two negative controls were run in every reaction: No Template and No Reverse Transcriptase. RT-qPCR was performed with a SsoFast EvaGreen Supermix kit with β-actin, β-tubulin, and GAPDH evaluated as reference genes (**Table 2.1**). Genes of interest that were tested are as following: Interleukin (IL) -4, IL-10, interferon gamma (IFNγ), transforming growth factor beta 2 (TGF-β2), tumor necrosis factor alpha (TNF-α), E-Cad, and PAFR (**Table 2.1**), Individual genes were optimized for both annealing temperature and concentration.

Table 2.1 Primer List of Human Genes for RT-qPCR

Gene	**Forward Primer (5' to 3')**	**Reverse Primer (5' to 3')**
IL-4	CTCACATTGTCACTGCAAATC	CTCTGTGAGGCTGTTCAAAG
IL-10	GACTTTAAGGGTTACCTGGGTTG	TCACATGCGCCTTGATGTCTG
IFNγ	TCGGTAACTGACTTGAATGTCCA	TCGCTTCCCTGTTTTAGCTGC
TGF-β2	CAGCACACTCGATATGGACCA	CCTCGGGCTCAGGATAGTCT
TNF-α	CAATAGGCTGTTCCCATGTAG	CACTGAATAGTAGGGCGATTAC
E-Cad	ATTTTTCCCTCGACACCCGAT	TCCCAGGCGTAGACCAAGA
PAFR	GATAGAGGTAGACTGGGTTAGG	GTCAGAGAAGGTTCCATCAAG
β-Actin	CGGGACCTGACTGACTAC	GAAGGAAGGCTGGAAGAG
β-Tubulin	ACCAACCTACGGGGATCTGAA	TTGACTGCCAACTTGCGGA
GAPDH	CACCATCTTCCAGGAGCGAGATC	GCAGGAGGCATTGCTGATGATC

The RT-qPCR program was as following: 95 °C × 30 seconds (s) + (95 °C × 5 s + 58 °C × 5 s + plate reading) × 40 cycles + melting curve. The melting curve step was a plate read every 0.5 °C increase from 65 °C to 95 °C with a stop every 2 s. Each RT-qPCR experiment was performed with a Bio-Rad CFX 96 real time system C1000 Touch thermal cycler. All RT-qPCR protocols were done in accordance with the MIQE guidelines **[152]**. Data analysis was performed with the Bio-Rad CFX Manager 3.1 software using the ΔΔCq method. The primer sequences are listed in **Table 2.1**.

2.7. Data Analysis

For the calculation of % viability, fold change and % change values, each value was divided by corresponding control value accordingly. To obtain the normalized % change value for Western Blot assay, each value was first normalized to the reference protein, β-tubulin, then divided by corresponding control value.

The statistical analysis of results was carried out using a two-tailed Student's t-test unless otherwise stated. Each experiment was conducted in at least three times, in triplicates. Results were interpreted using the mean ± SEM and the level of statistical significance. The significance is shown with $p < 0.05$ (*), $p < 0.01$ (**), $p < 0.001$ (***).

Chapter 3: Results

3.1. NP aerosols Generation and Characterization

The optimal condition for the generation of 5 nm sized Cu-based NP aerosols was achieved at approximately 3,600 V and 0.40 mA. The size distribution of NP aerosols measured by SMPS showed that the distribution followed Gaussian distribution and was monodispersed with GSD less than 1.6 in accordance with the literatures **[147-150]**. Although a perfectly monodisperse distribution has a GSD of 1.0 **[147]**, it is considered to be a monodisperse distribution with GSD up to 2.0 **[149]**. A size and number concentration of Cu NPs aerosols is presented in **Figure 3.1.1.**

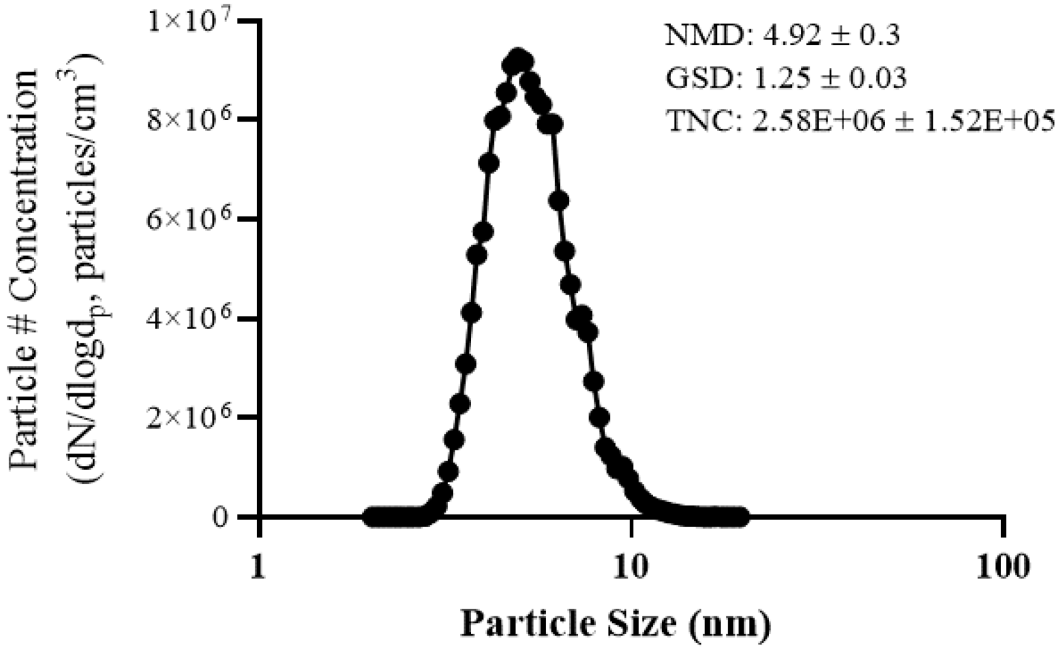

Figure 3.1.1 Representative size distribution and total number concentration of Cu NPs produced using the Spark Discharge System (SDS). The data was collected using Scanning Mobility Particle Sizer (SMPS) consist of nano Differential Mobility Analyzer (DMA) and Condensation Particle Counter (CPC).

NMD: number median diameter; GSD: geometric standard deviation; TNC: total number concentration

3.2. Cellular Response to Cu NPs Exposure (Objective 1)

3.2.1. Cellular uptake of Cu NPs

Following 4-hour ALI Cu NPs delivery, intracellular Cu ion level was measured using PG fluorescent dye. The PG fluorescence is quenched in the presence of cations, therefore, if A549 cells had taken up the Cu from the exposure, it was predicted that there would be a decrease in the fluorescence unit. As expected, when compared to the control, 4-hour ALI Cu NPs exposure group showed 49.5% decrease in the PG fluorescence (**Figure 3.2.1**), suggesting an increase in the presence of intracellular di-cations.

Although PG assay is often used for change in ion concentration, this assay has a limitation when used for Cu uptake specifically. Since the PG fluorescence is quenched with Cu ions, as well as Fe^{2+}, Ni^{2+}, Zn^{2+}. **[153]**, the delivery of Cu NPs to the cells needs to be confirmed to overcome this limitation. Previously in the lab, the total concentration of Cu^{2+} delivery was measured using Inductively Coupled Plasma-Mass Spectrometry (ICP-MS). When compared to control, 4-hour ALI Cu NPs exposure group showed significant increase in the total Cu concentration from cells exposed to Cu NPs compared to the cells exposed to Cu NPs-free air. Therefore, in conjunction with ICP-MS data, the decrease in PG fluorescence from **Figure 3.2.1** suggests that in response to ALI Cu NPs exposure, there is a significant increase in the intracellular Cu concentration.

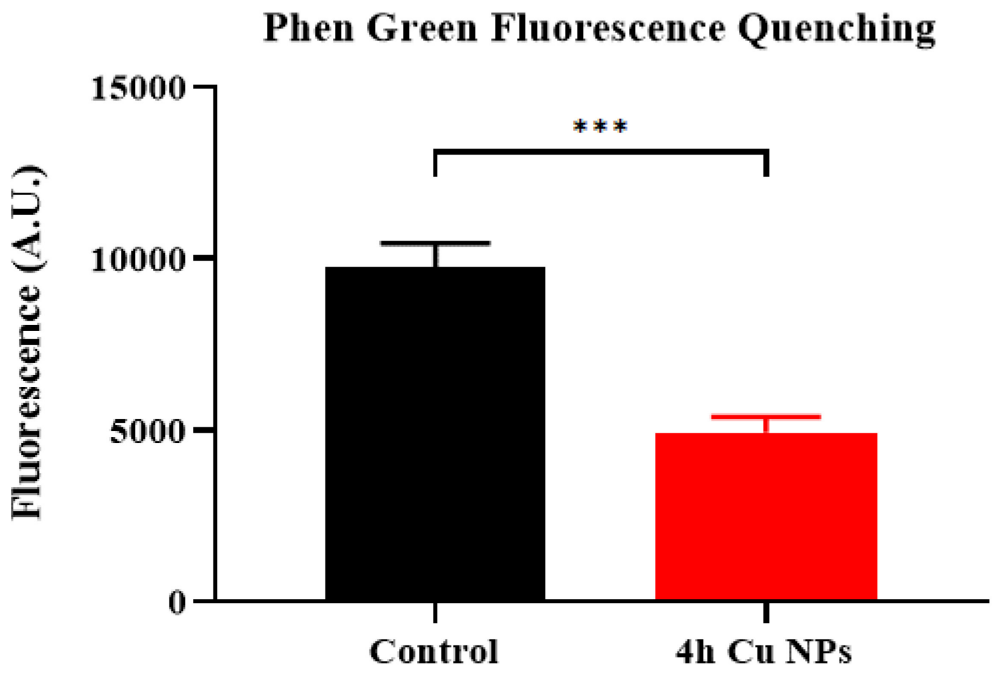

Figure 3.2.1 Intracellular cation quenching assay for control (Incubator) and 4h Cu NPs exposure groups for A549 cells using ALI exposure system using Phen Green SK assay. A549 cells were treated with PG fluorescence for 1 hour prior to the exposure. Cells were lysed with 0.5% Triton X-100 in PBS. Fluorescence was measured at 490/530 nm.

3.2.2. Cell viability

Once the uptake of Cu NPs by A549 cells was confirmed, the cellular response to the Cu NPs exposure was investigated. The cell viability was measured to test cytotoxicity of Cu NPs exposure. NP-free air exposure (NPs filtered with the HEPA filter), as described previously, was used as a control for ALI exposure. As the current ALI exposure system controls the temperature of the exposure chamber, but not the temperature and humidity of the aerosols used for the delivery of NPs, a slight decrease in cell viability in NP-free air exposure is expected **[156]**. Therefore, the use of particle-free air exposure (only filtered NPs) can confirm cytotoxicity of only Cu NPs exposure.

When using the ALI system for the exposure, there was no significant decrease in NP-free air exposure compared to the control. However, when cells were exposed to 2-hour and 4-hour Cu NPs, there were significant decrease in cell viability, 77% and 71%, respectively. This significant decrease in cell viability between 2-hour and 4-hour Cu NPs suggests that Cu NPs exposure induces cytotoxicity in dose-dependent manner.

As described previously, many studies investigating the toxicity of metal NPs suggest that cytotoxicity induced by metal NPs exposure is mediated by the production of ROS. Therefore, to investigate the mechanism of cytotoxicity of Cu NPs, cells were treated with the ROS scavenger, NAC, prior to exposure. The cytotoxicity observed in Cu NPs exposure was ameliorated with NAC treatment. The reduction in cell viability of 4-hour Cu NPs exposure group changed significantly, from 71% to 83% when treated with NAC, suggesting protection from cytotoxicity induced by Cu NPs. The viability of cells exposed to Cu NPs and NP-free air using the ALI exposure is shown in **Figure 3.2.2**.

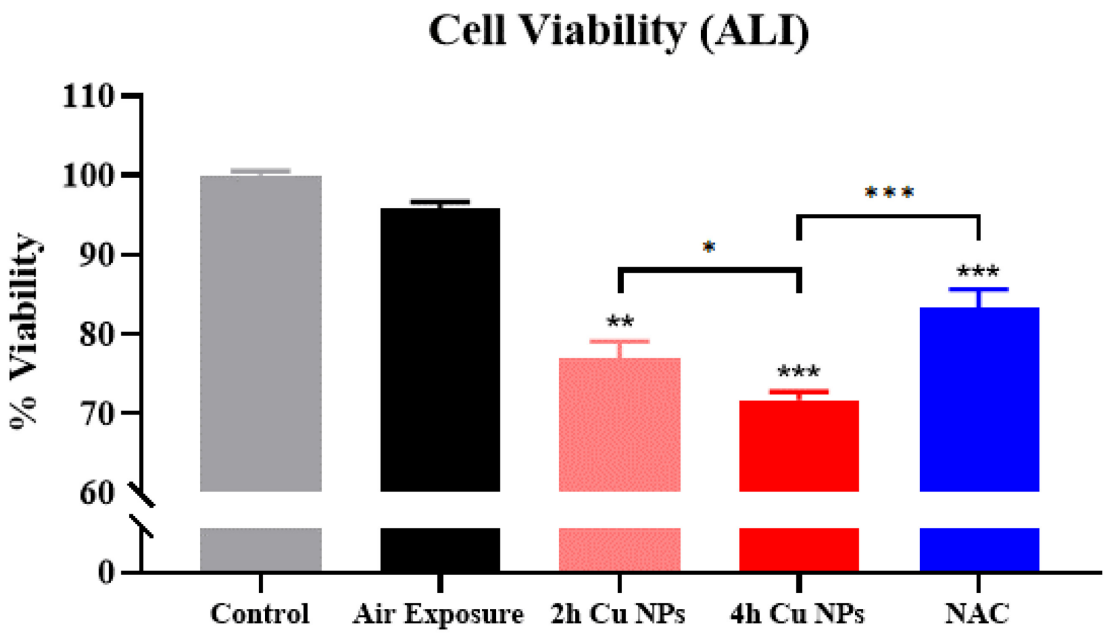

Figure 3.2.2 Cell viability for Control (Incubator), Air Exposure, 2h, 4h Cu NPs exposure and NAC treatment for A549 cells measured by MTT assay. Following the ALI exposure, cells were treated with MTT dye for 2 hours, then lysed with DMSO. The absorbance value was read at 562 nm and normalized to the control to obtain % viability. Air exposure is used as a control for statistical analysis unless otherwise indicated.

For the submerged exposure, the EM collected from the corresponding ALI exposure was used to culture A549 cells. Similar trend was observed with submerged exposure groups as ALI exposure. There was no significant decrease in cell viability from control to air exposure, with only 3% decrease. When cells were exposed to 4-hour Cu NPs exposure media for 24 hours, there was significant decrease in cell viability to 80% compared to the control. When treated with NAC, the viability was significantly increased compared to Cu NPs alone, suggesting lessening of cytotoxic effect as observed in the ALI exposure. The viability pf A549 cells exposed in EM for submerged exposure is shown in **Figure 3.2.3.**

As hypothesized, cells treated with NAC prior to 4-hour Cu NPs exposure showed an observable protection against the cytotoxicity induced by Cu NPs in both ALI and submerged exposures. Since NAC is the ROS scavenger, this suggests that the toxic effect by Cu NPs is ROS-mediated, this is also in accordance with literatures **[139, 157, 158]**.

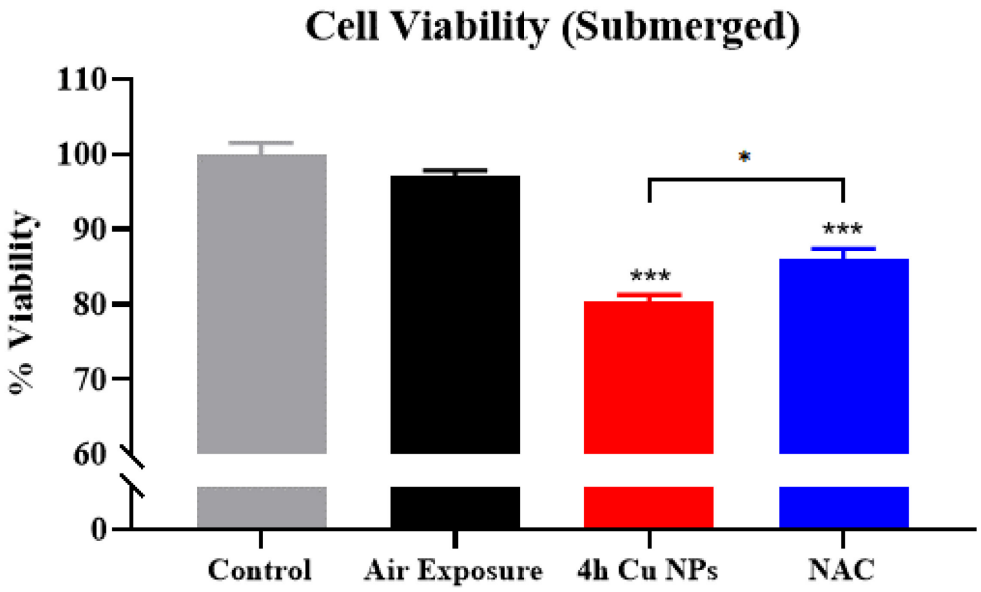

Figure 3.2.3 Cell viability for Control (Incubator), Air Exposure and 4h Cu NPs exposure and NAC treatment for A549 cells measured by MTT assay. A549 cells were exposed to corresponding Cu NPs exposure media for 24 hours. Following the exposure, cells were treated with MTT dye for 2 hours, then lysed with DMSO. The absorbance value was read at 562 nm and normalized to the control to obtain % viability. Air exposure is used as a control for statistical analysis unless otherwise indicated.

3.2.3. Intracellular ROS level

To confirm that the Cu NPs toxicity is induced by increased generation of ROS, intracellular ROS level was directly measured following ALI and submerged exposures. When A549 cells were exposed to NPs-free air using ALI exposure system, there was no significant difference observed compared to control with 1.05-fold generation of ROS. For 2-hour and 4-hour Cu NPs, there was observable and significant increase with 1.47 and 1.74-fold change in ROS level, respectively. As seen in cell viability data, the stepwise elevation of ROS generation in response to 2-hour and 4-hour Cu NPs exposure suggests a dose-dependent effect of Cu NPs. When treated with NAC, the elevated ROS generation was restored back to 1.18-fold change with no observable or significant change compared to air exposure. As expected, there was significant decrease in the ROS generation level when treated with NAC compared to 2-hour and 4-hour. This data supports that the cytotoxicity induced by Cu NPs exposure to A549 may be due to the elevated production of intracellular ROS. The intracellular ROS generation data is presented in **Figure 3.2.4**.

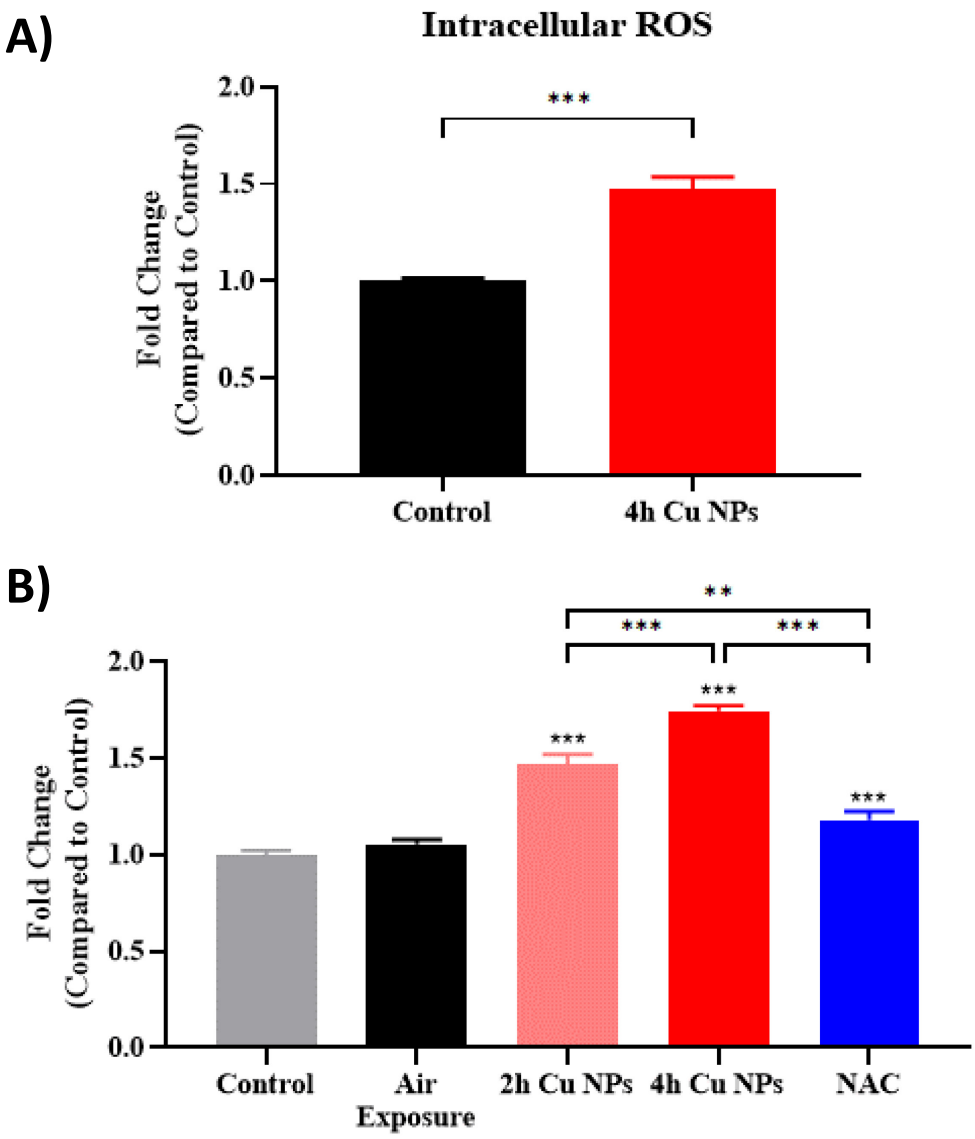

Figure 3.2.4 Intracellular ROS level for Control (Incubator), Air Exposure, 2h, 4h Cu NPs exposure, and NAC treatment following **(a)** submerged exposure, **(b)** ALI exposure measured with Carboxy-H2DCFDA. Following the exposure, cells were incubated with ROS dye, Carboxy-H2DCFDA, for 30 min, then lysed with 0.5% Triton X-100 in PBS. The fluorescence was read at 485/530 nm. Air Exposure was used as a control for statistical analysis when available unless otherwise indicated. All values were normalized to the control to obtain the fold change.

3.3. Bacteria Adhesion of *S. pneumoniae* (Objective 2)

3.3.1. *S. pneumoniae* 4 validation

Upon receipt of the bacteria from Dr. Jason LeBlanc's lab, *S. pneumoniae* 4 was tested for growth condition and counting. Although TSA II Blood Agar plate was commonly used to culture *S. pneumoniae* 4 in the lab, the liquid culture method was yet to be established. Several liquid broths were tested to develop optimal growth condition for *S. pneumoniae* 4; however, blood broth was avoided due to its storage restrictions. Among broths used were Brain Heart Infusion with and without 10% FBS, Muller Hinton Broth and TS) as recommended by literatures **[162, 163]** and ATCC. TSB showed the most increase in OD600 value over 24-hour period, thus was used for liquid culture of *S. pneumoniae* 4 from there on.

Based on the graph presented in **Figure 3.3.1**, the lag phase of the growth can be found between 0 h to 12 h, exponential phase between 12 h to 18 h, and stationary phase between 18 h to 24 h. For further experiments, 16 h point was selected to ensure that the infection was conducted with a consistent number of *S. pneumoniae* 4 at exponential phase.

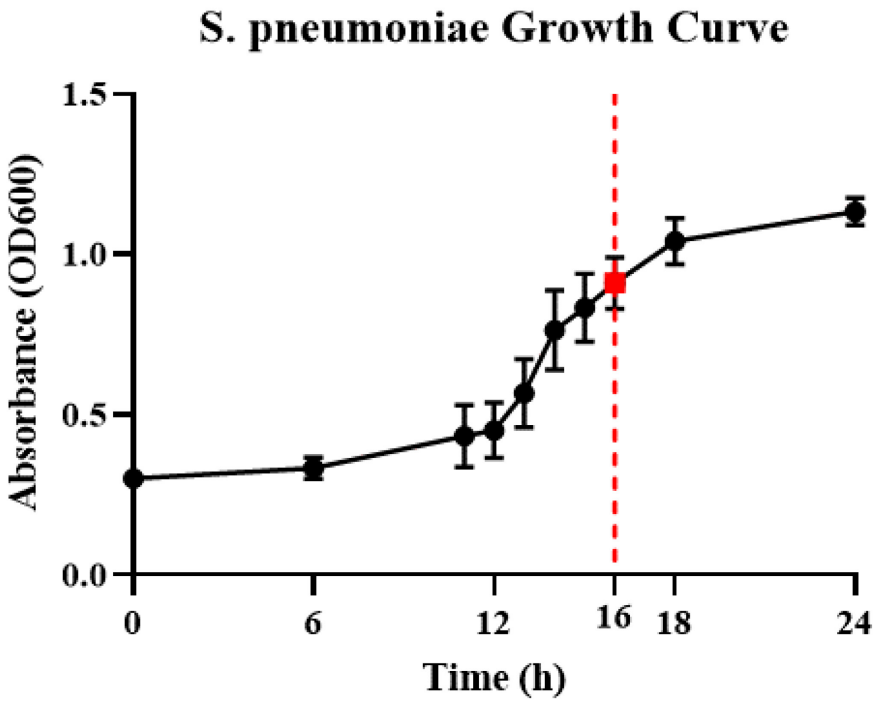

Figure 3.3.1 *Streptococcus pneumoniae* serotype 4 growth curve. Bacteria was cultured on TSA II blood agar plate for 24 hours prior to liquid culture. Bacteria inoculum was suspended to 10 mL of TSB culture media, then incubated at 37 ºC humidified environment with 5% CO_2. OD600 was measured using fresh TSB culture media as control.

In order to convert the OD600 values to total number of bacteria, OD600 versus CFU curve was created. The regression graph was created based on values obtained as described in the method section. Using the equation from the graph, the conversion of the OD600 of 1.0 is equivalent to 7.53E+08 CFU/mL. This conversion was used for the following bacterial infection studies. OD600 versus CFU graph is shown in **Figure 3.3.2**.

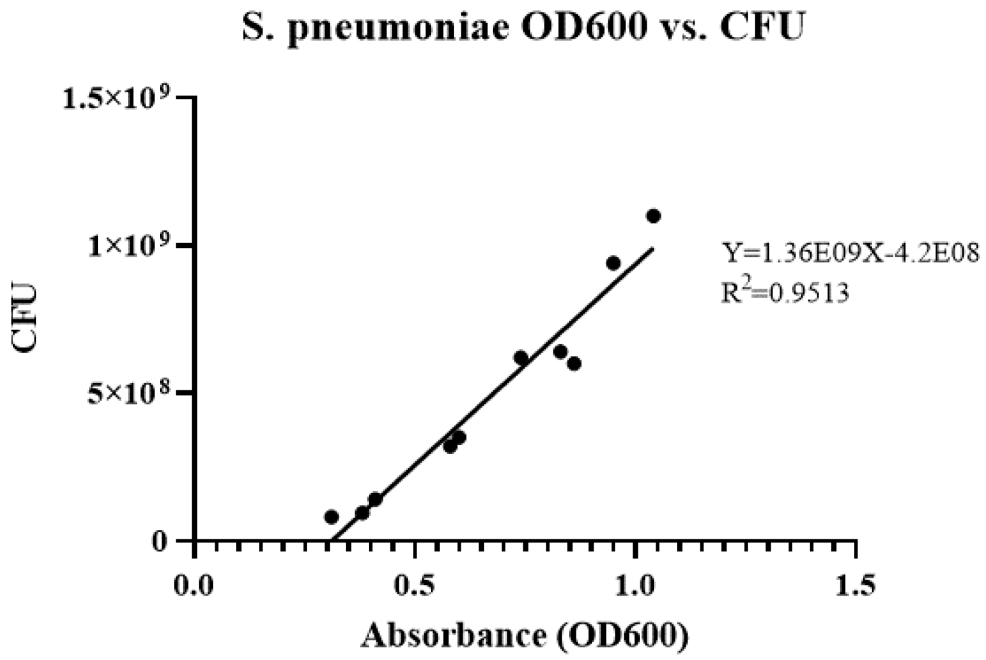

Figure 3.3.2 *Streptococcus pneumoniae* serotype 4 OD600 vs. CFU. Following OD600 measurement, serial dilution was conducted using PBS on TSB media containing bacteria. Each dilution was plated on TSA II blood agar plate. Plates were incubated at 37 ºC humidified environment with 5% CO_2 for 24 hours prior to CFU counting. Linear regression was forced through the origin. It has the slope of Y=1.36E09X-4.2E08, R^2 value of 0.9513.

3.3.2. Bacteria adhesion

It was hypothesized that A549 cells exposed to Cu NPs are more susceptible to infection by *S. pneumoniae* 4. Although *S. pneumoniae* is extracellular bacterial pathogen, it is also known to be highly invasive **[164]**. As bacteria adhesion to host cell is the first step during bacterial infection **[100]**, bacteria adhesion assay was used to measure the number of bacteria adhered to and internalized the host A549 cells to predict the level of infection by *S. pneumoniae* 4 on A549 cells. Following 2-hour and 4-hour ALI Cu NPs exposure, CFU count was significantly increased by 73% and 97%, respectively. This increase suggests that exposure to Cu NPs makes one more susceptible to bacterial infection, and that it follows dose-dependent pattern. As intracellular ROS level was elevated following Cu NPs exposure, it was hypothesized that treatment with NAC would be effective in attenuating the increased susceptibility to bacterial infection. As hypothesized, this increase was attenuated when treated with NAC, to 15% increase, where there was no statistical significance observed compared to air exposure. Bacteria adhesion data with ALI exposure is shown in **Figure 3.3.3**.

Similar pattern was observed in the submerged exposure samples. Following submerged exposure to 4-hour Cu NPs exposure media, CFU count was increased to 205% compared to control, and when treated with NAC, it was reduced to 122%. Submerged exposure bacteria adhesion data is shown in **Figure 3.3.4**.

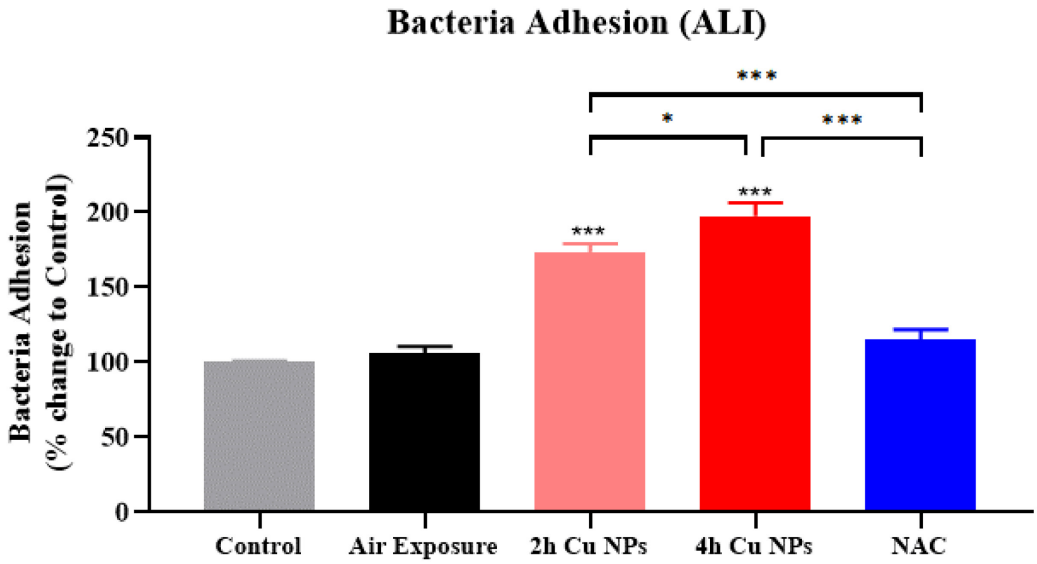

Figure 3.3.3 Bacteria adhesion level for Control (Incubator), Air Exposure, 2h, 4h Cu NPs exposure and NAC with Cu NPs exposure for A549 cells following ALI exposure. Following the ALI exposure, cells were infected with S.p4 at MOI of 10 for 2 hours. Following the infection, cells were lysed with 0.1% Saponin in PBS, diluted with PBS by 100-fold, then plated on TSA II blood agar plate overnight. CFU number was calculated and normalized to the control to obtain % change value. Air exposure was used as a control for statistical analysis unless otherwise indicated.

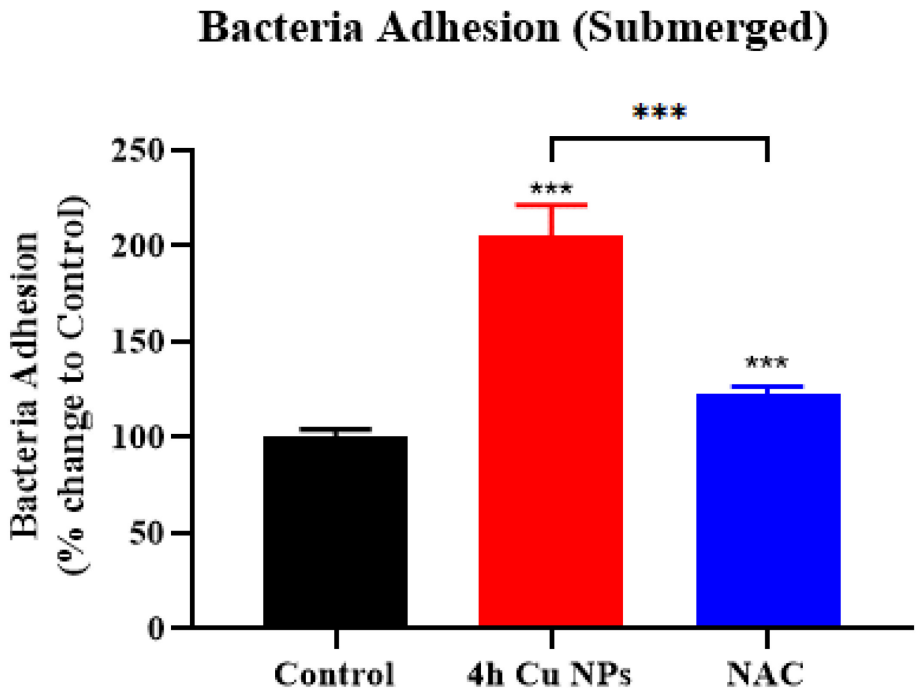

Figure 3.3.4 Bacteria adhesion level for Control (Incubator), 4h Cu NPs exposure and NAC treatment for A549 cells following submerged exposure. A549 cells were exposed to corresponding Cu NPs exposure media for 24 hours. Following the submerged exposure, cells were infected with S.p4 at MOI of 10 for 2 hours. Following the infection, cells were lysed with 0.1% Saponin in PBS, diluted with PBS by 100-fold, then plated on TSA II blood agar plate overnight. CFU number was calculated and normalized to the control to obtain % change value. Control was used as a control for statistical analysis unless otherwise indicated.

When 4-hour Cu NPs exposure bacteria adhesion data is corrected to cell viability, ALI exposure group shows 137% increase and submerged group shows 135% increase. This suggests that Cu NPs exposure increases susceptibility of bacterial infection in both ALI and submerged exposure condition to the similar extent

3.4. Host Surface Receptor and Cytokine Expression (Objective 3)

3.4.1. Protein expression by Western Blot

With the supporting data that Cu NPs exposure increases susceptibility to *S. pneumoniae* 4 infection, the mechanism behind the enhanced susceptibility was then investigated. As described above, the host-pathogen interaction is mediated by surface protein and receptor. In this study, the expression level of PAFR and E-Cad were investigated.

The relative protein level was measured using Western Blot assay. For E-Cad, there was observable decrease in air exposure group compared to control. This could be due to the fact that ALI culture presents less tight membrane junctions compared to conventional culture. One study by Ohlinger et al. compared the transepithelial electrical resistance (TEER) values between the ALI culture and submerged culture, to compare the monolayer integrity. The TEER values for the ALI culture was significantly lower than that of submerged culture, suggesting less tight junction on membrane in the ALI culture **[144]**. This could be explained by less expression of E-Cad in air exposure group as shown in **Figure 3.4.1**. Compared to air exposure, there was no statistical significance observed; however, there was observable difference when exposed to Cu NPs for 4 hours. Cells treated with NAC showed restoration of the expression level to the similar level as air exposure.

For PAFR expression, there was little difference between control and air exposure, and significant difference was observed with 4-hour Cu NPs exposure, where there was 73% increase in expression level. This increase in PAFR expression was restored to the same level as air exposure when treated with NAC. This data suggests that in response to Cu NPs exposure through ALI system, the protein expression level of both E-Cad and PAFR are increased, to a greater extent in PAFR than E-Cad, and this increase may be due to increased generation of ROS as NAC treatment was able to ameliorate the effects of Cu NPs exposure.

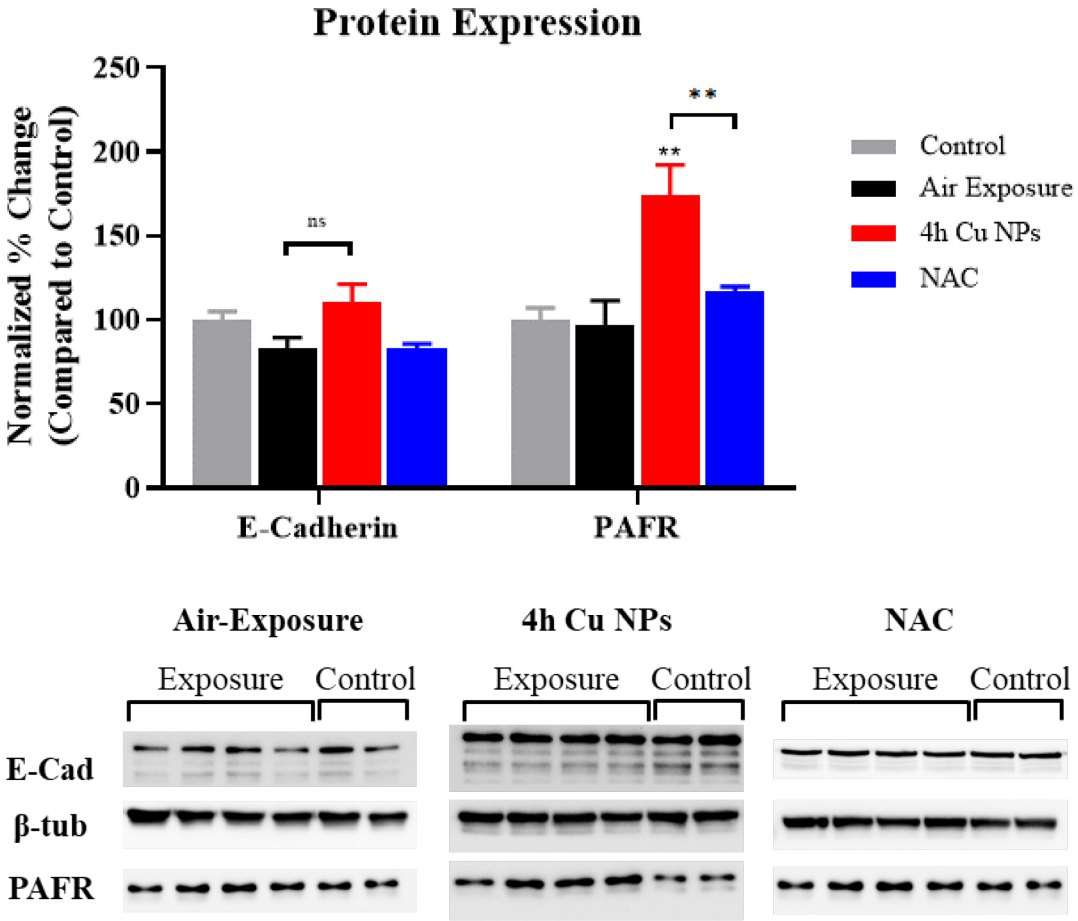

Figure 3.4.1 Normalized protein expression level of E-Cadherin and PAFR for Control (Incubator), Air Exposure, 4h Cu NPs exposure and NAC treatment following ALI exposure using Western Blot. β-tubulin was used as loading control. All values were normalized to the control to obtain % change value. Air exposure was used as control for statistical analysis unless otherwise stated.

3.4.2. Gene expression by RT-qPCR

To confirm the findings by Western blot, mRNA expression levels of both E-Cad and PAFR were measured using RT-qPCR. For reference genes, β-Actin, β-Tubulin and GAPDH were used. Using Bio-Rad CFX Manager 3.1 software, all three genes were in optimal range for usage as reference genes. When ΔΔCq method was used to measure the gene expression level, unlike protein expression level, both E-Cad and PAFR were significantly increased in dose-dependent manner compared to air exposure. With treatment of NAC, the increased expression was attenuated to the similar level as air exposure group. Gene expression level of E-Cad and PAFR are shown in **Figure 3.4.2**. This data, in conjunction with protein expression data, suggests that the Cu NPs exposure induces upregulation and increased expression of E-Cad and PAFR, which is associated with elevated susceptibility to bacterial infection by *S. pneumoniae.*

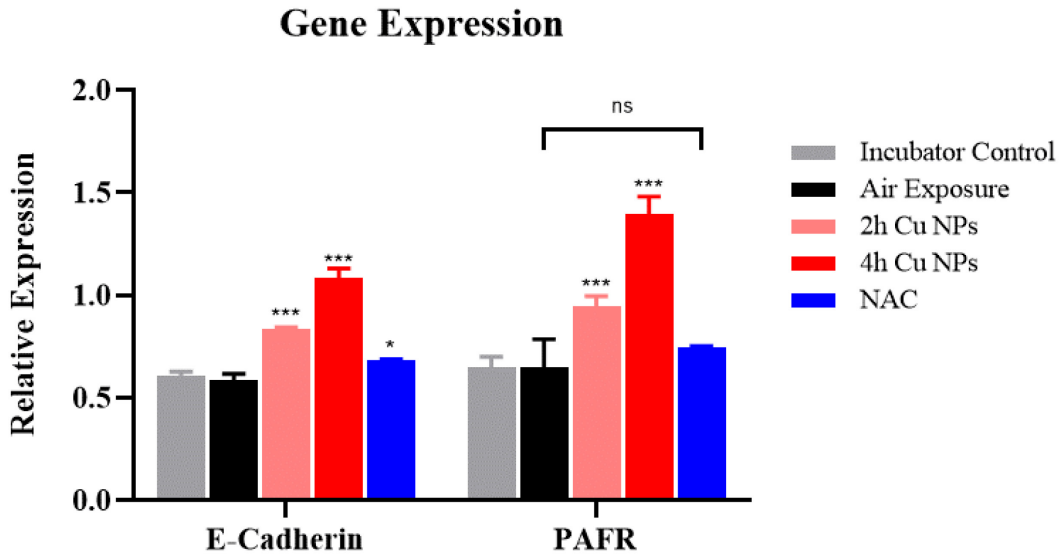

Figure 3.4.2 Surface receptor gene expression level of E-Cadherin and PAFR for Control (Incubator), Air Exposure, 2h, 4h Cu NPs exposure and NAC treatment following ALI exposure using RT-qPCR. β-actin, β-tubulin and GAPDH were used as reference genes. Data was analyzed using the Bio-Rad CFX Manager 3.1 software using the ΔΔCq method. Air exposure was used as control for statistical analysis unless otherwise stated.

As E-Cad and PAFR were confirmed to be expressed more when exposed to Cu NPs, further study was conducted to investigate the expression of cytokines involved in upregulation of these receptors. TGF-β2, TNF-α and IFNγ expression levels were measured as they were proposed to be involved in pathways upregulating the expression of PAFR **[172-174]**. For E-Cad, IL-4 and IL-10 were measured **[175, 176]**. Same genes were used as reference genes as above. Upon completion of analysis, TNF-α was the only gene showing observable and significant difference in dose-dependent manner when exposed to 2-hour and 4-hour Cu NPs exposure. Similar trend, though not significant, was observed in Cu NPs exposure group of of IL-4, IL-10, and IFNγ. As for TGF-β2, there was slight decrease as opposed to other genes tested. The gene expression data for of IL-4, IL-10, TGF-β2, TNF-α and IFNγ are shown in **Figure 3.4.3**.

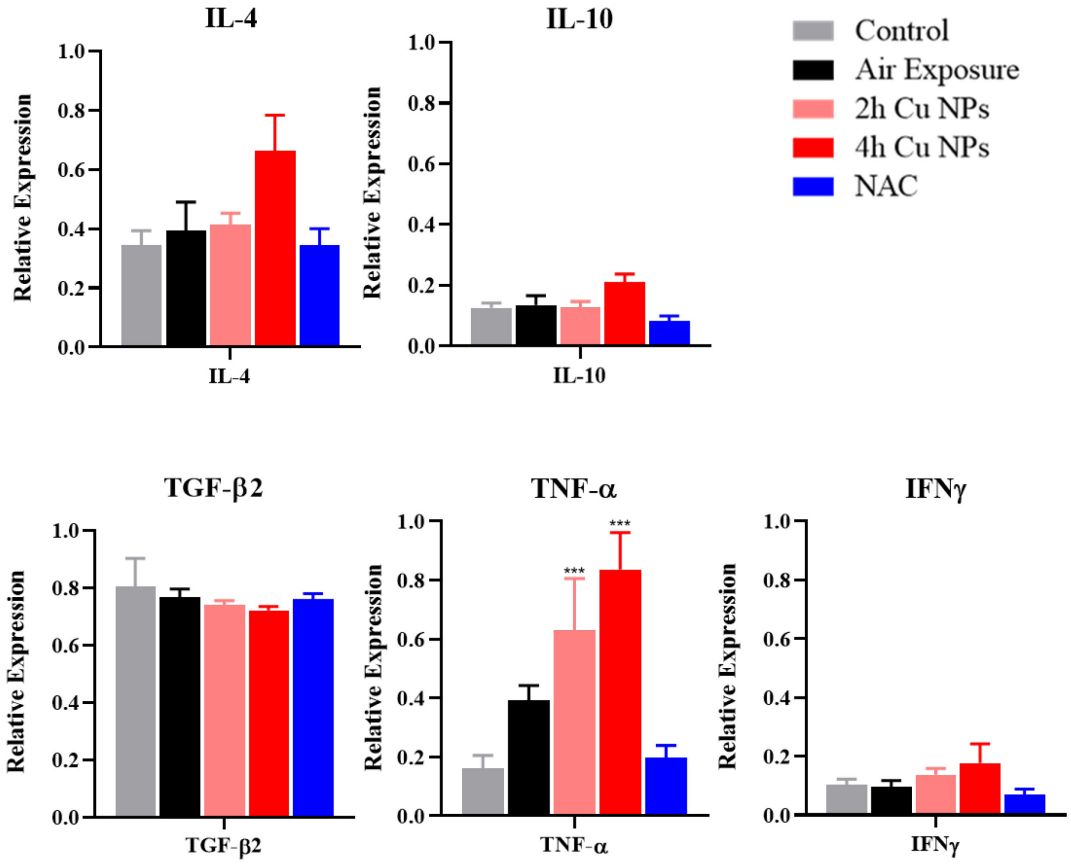

Figure 3.4.3 Gene expression level of IL-4, IL-10, TGF-β2, TNF-α and IFNγ for Control (Incubator), Air Exposure, 2h, 4h Cu NPs exposure and NAC treatment following ALI exposure using RT-qPCR. β-actin, β-tubulin and GAPDH were used as reference genes. Data was analyzed using the Bio-Rad CFX Manager 3.1 software using the ΔΔCq method. Air exposure was used as control for statistical analysis unless otherwise stated.

Chapter 4: Discussion

4.1. Cytotoxicity of Cu NPs Exposure

Exposure risk of Cu NPs has been studied by many researchers, and its toxicity has been characterized through both *in vivo* and *in vitro* studies. Many *in vitro* studies used traditional submerged exposure system. While the use of submerged exposure is standard in toxicology studies, a better *in vitro* exposure system mimicking *in vivo* conditions is available. As described previously, the ALI exposure system offers exposure set up that reflects the physiological condition of pulmonary system more accurately. Therefore, this study aims to verify the findings of submerged exposure system and provide insight into mechanism behind enhanced bacterial infection induced by Cu NPs exposure.

The use of SDS for NPs generation and continuous monitoring system allowed for controlled and monodispersed aerosol generation of Cu NPs. In conjunction with the ALI exposure system, the experimental set up used in this study presents great value in that it allows uniform, efficient and dose-controlled delivery of Cu NPs to cells.

The cytotoxic effect observed in this study is of lesser extent compared to other study conducted with similar set up. Jing et al. have reported in response to 4-hour Cu NPs exposure, there was 40% cell viability. When compared to cytotoxicity observed in the current study, 71% viability, the cytotoxicity reported by Jing et al. seems much more severe **[139]**. It could be attributed to the fact that the size and concentration of Cu NPs used for this study are lower. In this study, the median diameter was 4.9 nm and the concentration was 2.58E+06, which were lower when compared to similar study conducted by Jing et al., where the median diameter was 9.2 nm and concentration 2.27E+07 **[139]**. Smaller sized particles are known to offer greater toxicity as they can

reach alveolar region **[61, 62]**. A study conducted by Soares et al. evaluated the size-dependent cytotoxicity of silver (Ag) NPs **[62]**. 10 nm and 50 nm sized Ag NPs were compared and based on several cell viability assays, and the authors noted that exposure to 10 nm Ag NPs induced greater cytotoxicity as well as membrane damage when compared to that of 50 nm Ag NPs.

Lower concentration also offers a better representation of real-life exposure scenarios. While many *in vitro* studies typically use high concentration for acute exposure scenarios, real-life exposures are often chronic (repeated low-dose) exposure **[177]**. High-dose NPs exposure may lead to greater toxicity, but low-dose exposure provides more relatable information to the real-life exposure scenarios. Additionally, to observe dose-dependent response to NPs exposure, varying time points, 2-hour, and 4-hour, were also implemented in this study. Based on the study by Soares et al., it was also noted that increasing concentration and duration of Ag NPs exposure led to step-wise decrease in cell viability, suggesting dose-dependent cytotoxicity as well **[62]**. Therefore, the smaller size and lower concentration as well as implementation of different duration in this study offers more realistic information to real-life exposure scenarios, namely occupational exposures.

As hypothesized, Cu NPs exposure to A549 using SDS NPs generation and the ALI exposure system displayed dose-dependent cytotoxicity. The Phen Green assay in conjunction with previously conducted ICP-MS data confirmed the uptake of Cu NPs by A549. Cytotoxicity of Cu NPs were confirmed with MTT assay, where dose-dependent decrease in cell viability was observed in 2-hour and 4-hour Cu NPs exposure. When treated with ROS scavenger agent NAC, the cytotoxicity was attenuated, with increased

cell viability similar to air exposure level. As expected when the intracellular ROS was measured, there was dose-dependent increase in ROS generation confirming that the cytotoxicity observed in Cu NPs exposure is likely due to the increased ROS generation and subsequent increase in oxidative stress, leading to cell death.

4.2. Cu NPs Exposure Enhances Susceptibility to *S. pneumoniae* Infection

Based on the growth curve of the *S. pneumoniae* 4, 16-hour culture was selected, which is later than the mid-exponential phase. In bacteria study, mid-exponential phase is commonly used as it ensures the constant growth rate and uniform metabolic activity of bacteria. However, since *S. pneumoniae* is preferably cultured on blood agar plate, there is a limitation that the growth rate on agar plate is different than that of liquid culture. A review on the growth of bacterial colony by Jeanson et al. has suggested that the slower growth is observed in colony growth than in liquid culture, and that it can be due to the limited access to nutrient as bacteria are immobilized **[178]**. Therefore, the use of 16-hour point would ensure that *S. pneumoniae* used for this study is in the exponential phase of the growth.

Evidence provided by studies support that workers exposed to welding fume are at higher risk to bacterial infection by *S. pneumoniae* **[87, 91, 130]**. As Cu NPs is commonly found in welding fume **[179]**, and widely used in industrial applications, it is important to understand the link between Cu NPs and *S. pneumoniae* infection to characterize and prevent health risks. Additionally, causal relationship between Cu NPs and *klebsiella pneumoniae* infection was proposed by Kim et al. **[145]** with *in vivo* study. Taken together, there is strong evidence that Cu NPs induces enhanced susceptibility to

S. pneumoniae infection.

As hypothesized A549 exposed to Cu NPs showed dose-dependent increase in bacterial adhesion. The increased susceptibility to bacterial infection, which was previously investigated by others in the lab using *in vitro* submerged exposure system, was confirmed using the ALI exposure system. Interestingly, treatment with NAC has led to decrease in bacteria adhesion level in response to Cu NPs exposure. This data suggests that the enhanced susceptibility may be linked to the inflammation and oxidative stress as well.

Unlike the cell viability data, bacteria adhesion data showed increased effect of Cu NPs in submerged exposure than ALI. This could be attributed to the fact that following the exposure, more viable cells are present for bacterial infection study in submerged exposure compared to ALI. As the bacteria infection is conducted under the assumption that the same number of A549 cells are present on all samples, submerged exposure with lesser cell death would evidently show higher bacteria adhesion level compared to ALI exposure.

4.3. Cu NPs Exposure Alters Expression of Surface Proteins and Related Genes

As described previously, host surface receptors possess ability to interact with *S. pneumoniae* ligands and mediate adherence and invasion. There are multiple receptor-ligand interactions discovered for *S. pneumoniae* infection. Amongst which, the well-studied receptors are polymeric Immunoglobulin Receptor (pIgR), E-Cadherin and PAFR **[107, 165-167]**. pIgR plays an important role in host defense as pIgR is responsible for

transporting secretory component from basolateral side of mucosa layer to lumen, the apical side **[165]**. This secretory component has multiple functions as mucosal defense, which includes but not limited to non-specific microbial scavenger, neutralization of toxins and protection of secreted immunoglobulin **[165, 168]**. pIgR, however, is also known to bind to choline binding proteins on *S. pneumoniae* surfaces, widely studied adhesin expressed by *S. pneumoniae* **[165, 169]**. E-Cad is more known for its critical function as intercellular junctional protein, responsible for maintaining epithelial membrane integrity **[166, 170]**. Recent studies have identified the role of E-Cad in bacterial entry into host cells by gram-positive bacteria, and specifically for *S. pneumoniae,* it is proposed that E-Cad interacts with pneumococcal surface adhesin A (psaA), another widely studied adhesin **[166]**. As described in the introduction, PAFR is important receptors involved in host immune system. It has been also identified as a receptor responsible for binding with surface protein expressed on *S. pneumoniae* and facilitate adhesion and invasion into the host cell **[107, 108]**. Although these receptors are identified as part of *S. pneumoniae* infection, not all of them are expressed in distal respiratory region. Both E-Cad and PAFR are expressed by alveolar type II cell line, A549; however, pIgR is only expressed in upper respiratory tract **[171]**. Therefore, for this study, the levels of E-Cad and PAFR expression were investigated.

Based on the data obtained by Western Blot assay, the protein expression level of PAFR showed significant increase in response to Cu NPs exposure, and decreased to baseline when treated with NAC. E-Cad did not show any significance, but there was an observable difference in protein level. Gene expression data by RT-qPCR showed that both receptors were significantly increased in dose-dependent manner, and the increase

was attenuated when treated with NAC.

It was brought to my attention that while there was consistent result obtained between protein and gene expression in PAFR, E-Cad data showed significant increase only in gene expression. The fact that E-Cad showed significant increase in gene expression, but not in protein level could be explained by two potential reasons. First is that the expression of the E-Cad is slower than PAFR, as a result, the mRNA expression could be upregulated, but is yet to be translated into the proteins. Second potential theory is that the role of E-Cad is primarily creating healthy adherent junction between epithelial cell-to-cell contact **[180]**. As described previously, cells cultured in the ALI exposure system undergoes surface property changes to mimic the physiological pulmonary epithelial condition such as a production of surfactant **[144]**. The authors presented that when cultured in the ALI system, there is increased leakage compared to conventional culture, suggesting disruption in tight junction formation. Another contributing factor for little E-Cad protein expression is the nature of cell line used. For example, the cell line used in this study is A549, which is derived from human lung adenocarcinomas, and its intercellular adhesion is poor **[180]**. Since E-Cad is tumor suppressor gene, there is a limitation in the extent of characterization that can be done of E-Cad expression with the use of carcinomic cell line **[180]**. However, increase in gene expression of E-Cad observed is still a valuable finding. As this finding indicates that Cu NPs exposure triggers upregulation of E-Cad, which is not highly expressed in normal condition of A549.

Therefore, the protein/gene expression data provides convincing argument that the mechanism of Cu NPs induced enhanced susceptibility to *S. pneumoniae* infection is

mediated by upregulation of surface receptors, E-Cad and PAFR, which are responsible for bacterial infection.

Induction of cytokines in response to metal NPs exposure has been studied before. There is an array of cytokines that are upregulated. **[50]**. More specifically, Cu NPs exposure to bronchial epithelial cell line induced significant increase in Il-6 and Il-8 mRNA expression as well as mucus production **[181]**. It was proposed that the induction of pro-inflammatory cytokines was associated with activation of mitogen-activated protein kinases pathway, also known as MAPK pathway **[181]**. Evidence supports that the Cu NPs exposure leads to induction of cytokine production. Therefore, with confirmed upregulation of surface receptors, the involved pathways were investigated by observing cytokine productions.

To investigate the regulation of PAFR, TGF-β2, TNF-α, and IFNγ expressions were measured. TGF-β2 is known for its role as an immunomodulator, its activities include cell differentiation, antibody production and class switching of B cells **[172]**. As immunomodulator, its function in upregulation of PAFR had been studies as well. It was proposed that in response to TGF-β2, there was an increase in the binding of the nuclear factor to the PAFR gene transcript, leading to induction of gene expression **[172]**. TNF-α is another cytokine involved in PAFR expression. TNF-α is known to activate nuclear factor-κB pathway, and as PAFR gene promotor contains nuclear factor-κB sequences, TNF-α can upregulate PAFR through activation of nuclear factor-κB **[173]**. The relationship between IFNγ and PAFR upregulation was first reported in 1994. Although the mechanism of action was not elucidated, the study suggested that treatment with IFNγ leads to accumulation of PAFR mRNA, leading to increased expression **[174]**.

To investigate the regulation of E-Cad expression, IL-4 and IL-10 were tested. A study by Moreno et al. have proposed that the E-Cad upregulation is induced by IL-4 as part of macrophage activation. The author specified that the mechanism of induction by IL-4 is through STAT6 pathway **[176]**. Similarly, IL-10 is directly involved in upregulation of E-Cad as well. Recent study suggested that treatment with IL-10 led to increased expression of E-Cad and not any other adhesion molecules. It was proposed that the IL-10 downregulates microRNA-9, which inhibits the expression of E-Cad, resulting in upregulation of E-Cad **[175]**.

Upon completion of RT-qPCR gene expression experiment, there was observable increase in expression of IL-4, IL-10 as well as IFNγ, and significant increase in TNF-α. Interestingly, there was a decreasing trend observed in expression of TGF-β2, though not significant. This decrease could be explained by the complex function of TGF-β2, where both pro- and anti-inflammatory effects can be achieved in combination with other cytokines **[182]**. One of its function is tumor suppression. It was suggested that the down-regulation of TGF-β could result in tumor suppression via induction of apoptosis by tumor cells **[183]**. More specifically, using A549 cells, downregulation of TGF-β had led to decreased proliferation and induction of apoptosis **[184]**. As Cu NPs exposure dose used in this study is low, it is likely to lead to the apoptotic cell death rather than necrosis **[185]**. This can be further supported by the fact that TNF-α, known for its ability to induce inflammatory response and apoptosis, is significantly increased in response to Cu NPs exposure. TGF-β blockade has also been suggested to lead to an increased production of IFNγ **[182]**. Therefore, decreasing trend observed in TGF-β2 in response to Cu NPs exposure could be a result of the induction of apoptotic pathway, leading to

increased expression of IFNγ which is also observed in the current study.

However, the difference in gene expression observed in this study is very small. Even with significant difference observed in TNF-α group, the difference between the control and 4-hour Cu NPs exposure is only about 5-fold difference. Considering the nature of the RT-qPCR experiment, it can be argued that the difference needs to be bigger in order to present a meaningful information. However, an alternative explanation could be that the little increase in gene expression of cytokines could be attributed to the fact that since these cytokines are responsive early in detection of cellular damage, 2-hour and 4-hour time point may be too late to detect the expression level of these cytokine genes. As both E-Cad and PAFR gene upregulation as well as protein synthesis have already been completed, cytokine gene expression level detected at these time points could be a residual effect of Cu NPs.

One major limitation of this study is that the functionality test with PAFR and E-Cad antagonist has not been conducted. Although the increased expression of the surface receptors has been observed in both Western Blot and RT-qPCR, the functionality of the receptors was not investigated. The antagonist treatment study was planned; however, due to unforeseen circumstances, the experiment could not be reasonably carried out within the timeline.

Studies suggest that E-Cad interacts with bacterial lipoprotein psaA **[166, 186]**. However, in 2004 there was one paper disputing the role of psaA in bacterial infection by *S. pneumoniae* **[187]**. The authors proposed that since psaA is hidden beneath cell wall and polysaccharide capsule, it cannot directly interact with host receptors to mediate infection **[187]**. They also proposed that the loss of virulence in psaA mutated *S.*

pneumoniae is mediated by disruption of metal transport system, instead of loss psaA expression **[187]**. Since then, there was one study published on the functionality of E-Cad during *S. pneumoniae* infection. In 2007, Anderton et al. have proposed that the *S. pneumoniae* infection is indeed mediated by direct interaction between E-Cad and psaA **[166]**. Anderton et al. conducted functionality tests with upper airway tract cell line and psaA-coated fluospheres. In one experiment, cells were pretreated with anti-E-Cad antibody to block active sites of the receptor, subsequent co-incubation with psaA-coated fluospheres showed 46% decrease in adherence. In another experiment, anti-psaA antibody was used to block psaA on the fluospheres. After subsequent co-incubation, there was approximately 60% decrease in adherence **[166]**. With convincing evidence provided in this study, it is plausible that E-Cad is involved in infection pathway by *S. pneumoniae*. However, there was no further studies conducted in this subject. Therefore, a functionality test is necessary to confirm that the increased E-Cad expression in this current study mediates enhanced bacterial infection in response to Cu NPs exposure.

On the other hand, the role of PAFR in *S. pneumoniae* infection has been well studied over the years; however, to confirm that the upregulation of PAFR is indeed related to the enhanced bacterial infection, functionality tests need to be carried out. There are several studies that observes the expression level of PAFR in response to environmental and occupational exposures, namely a study by Mushtaq et al., **[109]** and Grigg et al. **[108]**. Mushtaq et al. has investigated the toxicity of exposure to urban particulate matter (<10 μm and <2.5 μm). In this study the exposure to these particulate matters induced upregulation of PAFR mRNA transcript, and when treated with PAFR antagonist, this toxic effect was attenuated **[109]**. Another study conducted by Grigg et al.

has investigated the relationship between cigarette smoke and increased risk of pneumococcal infection. In this study, the upregulation of PAFR was confirmed in response to cigarette smoke exposure. Additionally, cells were co-incubated with PAFR antagonist and the cigarette smoke exposure stimulated adhesion by *S. pneumoniae* was attenuated, suggesting the role of PAFR in bacterial infection **[108]**.

Although the functionality test can bring insight into the role of the PAFR in the infection pathway, there is enough convincing evidence supporting its involvement in infection pathway by *S. pneumoniae.* Therefore, this study elucidates that the enhanced bacterial infection risk associated with Cu NPs exposure is mediated by upregulation of surface receptors that interacts with *S. pneumoniae.*

There is a limitation in the experimental setup for the gene expression of cytokine. As cytokines studied are heavily involved in immune function, expression of these genes can be influenced by cell death. Since the cytotoxicity of Cu NPs exposure was shown in **Figure 3.2.2**, it can be argued that the change in expression of cytokines observed can be due to the effect of cell lysates alone, independent from Cu NPs exposure. It has been suggested that low dose metal NPs exposure results in apoptotic pathway, while high dose NPs exposure results in necrotic pathway **[185]**. As stated previously, this study utilizes low dose and concentration of Cu NPs exposure compared to other studies. Therefore, the likelihood of apoptotic cell death is higher than necrotic death. Since many cytokines are involved in both cell death pathways, the observed change in gene expression could be a due to the activation of cell death pathways rather than Cu NPs alone.

This question could have been answered with employing a cell lysis control,

where cells are co-incubated with cell lysates, and by comparing the gene expression level with Cu NPs. However, there are couple of concerns regarding the use of cell lysis control. First, the concentration of cell lysates present in Cu NPs exposure group is unknown. Since the concentration of cell lysates are unknown in Cu NPs exposure, selecting a suitable concentration for cell lysis control becomes a problem. Too little lysates will not provide relevant comparison to Cu NPs effect, and too much lysates will potentially mask the effects induced by Cu NPs. Second, the reagents used to prepare cell lysates may be delivered to cell lysis control. There are various ways to prepare for cell lysate, such as antibody treatment, chemical treatment, and lysis buffer. Following lysis, lysates are collected by centrifugation. It is possible that residual lysis reagents are present and provide inaccurate information for cell lysis control.

In the study, air exposure was used as an ultimate control for Cu NPs exposure. As described in section 3.2.2, there is decrease in cell viability observed in air exposure. Although the extent of cell death observed in air exposure group is less compared to Cu NPs exposure, air exposure control does not use any other reagent apart from what's used in Cu NPs exposure, therefore it can be considered to function as cell lysate control when observing gene expression of cytokines. Use of air exposure does not disregard the significant information that can be provided by cell lysis control; however, in the absence of cell lysis control, air exposure can bring relevant information to draw conclusion on effect of Cu NPs on cytokine regulation.

4.4. Summary and Conclusion

The main objective of this study was to elucidate the mechanisms underlying the effect of

airborne Cu NPs exposure on enhanced bacterial infection using the *in vitro* NPs exposure model. The results presented in this study confirms the cytotoxicity of Cu NPs exposure, and enhanced susceptibility to *S. pneumoniae* infection using the ALI exposure system. These toxic effects of Cu NPs have been proposed to be mediated through increased ROS production and resulting elevated oxidative stress. Through evaluating the levels of protein and gene expressions, the underlying mechanism of enhanced bacterial infection is proposed to be mediated through upregulation of surface receptors, E-Cad and PAFR. Upon investigation of cytokine production involved in expression pathway of these receptors, there was significant increase in TNF-α, and observable increases in IL-4, IL-10 and IFNγ, while observable decrease in TGF-β2. These cytokines are known to be heavily involved in inflammatory pathways as well as immune response. As Cu NPs exposure leads to increased oxidative stress through the generation of intracellular ROS, the exposure to Cu NPs is expected to induce change in expressions of cytokines involved in both inflammatory and regulatory responses. Complex function of TGF-β2 could be attributed to the decrease observed in response to Cu NPs, as one of its functions includes regulatory response. According to literatures, IL-4 and IL-10 are involved in mediating the upregulation of E-Cad expression, and TGF-β2, TNF-α and IFNγ involved in upregulation of PAFR. Therefore, this provides evidence that Cu NPs exposure leads to upregulation of surface receptor expression leading to enhanced susceptibility to *S. pneumoniae* infection.

There is a growing concern of Cu NPs as this nanotechnology is applied and the number of products containing Cu NPs is growing exponentially. In order to utilize nanotechnology safely, extensive exposure assessment and toxicological studies for NPs

must be completed. Couple studies proposed the toxicity of Cu NPs and its relation to increased bacterial infection by *S. pneumoniae.* However, not many studies were conducted to investigate the mechanisms thereof. This study provides insight into characterizing the underlying mechanism of enhanced bacterial infection in response to Cu NPs exposure using *in vitro* ALI exposure system. In conclusion, this project has established cytotoxic effect of Cu NPs and enhanced bacterial infection by *S. pneumoniae.* Furthermore, this project elucidated potential mechanisms of *S. pneumoniae* infection, which is mediated by altered expression cytokines resulting in the upregulation of host surface receptors, PAFR and E-Cad.

4.5. Future Directions

4.5.1. Functionality test with surface receptor antagonists

The importance of a functionality test is as aforementioned. Previously, other studies have used antagonist for E-Cad and PAFR to prevent its interaction with *S. pneumoniae.* For E-Cad blocker, Anderton et al. have used anti E-Cad antibody to block the receptor activity **[166]**. For PAFR blocker, couple studies have used different types of PAFR antagonist, which are commercially available **[108, 109]**. Therefore, with completion of the functionality test, it can provide mechanistic insight into the role of E-Cad and PAFR in *S. pneumoniae* infection. Since studies with the role of E-Cad have not been explored as much as that of PAFR, this information can strengthen the conclusion of receptor expression being a key factor in Cu NPs-induced enhanced susceptibility to *S. pneumoniae* infection.

4.5.2. Cu NPs ALI exposure using different cells

As described previously, one of the major surface receptors responsible for meditating infection by *S. pneumoniae* is pIgR **[165]**. Since pIgR is highly expressed in the upper airway tract and decreases in its expression as it reaches respiratory region **[171]**, A549 cells used in this study is not able to capture the role of pIgR in enhanced bacterial infection induced by Cu NPs exposure. Therefore, use of upper airway tract cell line such as Detroit 562 (human nasopharyngeal cells), can provide insight into upper airway colonization and infection of *S. pneumoniae* in response to Cu NPs exposure.

4.5.3. Investigating the infection by other serotypes of *S. pneumoniae*

As described previously polysaccharide capsules of *S. pneumoniae* is an important virulence factor, and these capsules are expressed in different pattern in various serotypes of the *S. pneumoniae* **[121]**. Each serotype poses different level of community health issues with different epidemiological patterns. While *S. pneumoniae* 4 is most prevalent in several outbreaks in vulnerable populations and workers exposed to metal fumes such as welding fume, other serotypes are also responsible for outbreaks. While implementation of PCV13 has been effective in creating herd immunity, the serotypes covered by PCV13 are still persistent in causing community acquired pneumonia **[123]**. Specifically, serotype 3 is of concern. Many explanations were proposed to explain the persistence of serotype 3 *S. pneumoniae* even after the implementation of new vaccine schedule **[188]**. Specific reason for its persistence, however, remains to be studied. Therefore, understanding the effects of Cu NPs on other serotypes would provide valuable knowledge to the toxicity of Cu NPs, as well as *S. pneumoniae*.

4.5.4. Assessment of direct interaction between *S. pneumoniae* and Cu NPs

Cu NPs are well known for its antimicrobial activity, commonly used for coating of surfaces to prevent bacterial proliferation. However, the effect of Cu NPs on bacteria in its infectious capacity is not elucidated. Current study focuses on the effect of Cu NPs and the host cells primarily, as the infection with *S. pneumoniae* occurs subsequently, in the absence of Cu NPs in the surroundings. Since the current experimental set up limits and minimizes potential interaction between *S. pneumoniae* and Cu NPs, the direct interaction between Cu NPs and *S. pneumoniae* is not explored. It would be interesting to test the effect of Cu NPs on *S. pneumoniae* as it can potentially provide further insight into the toxicity of Cu NPs.

Cu NPs and bacteria interaction is possible to occur spontaneously. As *S. pneumoniae* is part of commensal flora and colonizes in human lungs, when inhaled, Cu NPs can interact with not only pulmonary epithelium, but also the colonized bacteria. A study by Johnson et al. 2015 proposed that an increased expression of Cu export system prior to the infection promotes more robust infection **[189]**. When export related genes were knocked out, it resulted in less virulent *S. pneumoniae* and they were more prone to macrophage-mediated clearance. As regulation of Cu export system is mediated by the surrounding Cu concentration **[190]**, Cu NPs exposure could lead to increased expression of this system leading to increased virulence of *S. pneumoniae.*

4.5.5. Effect of growth phase of *S. pneumoniae* in infection study

Conducting infection with *S. pneumoniae* in lag phase would be interesting as well. A study by Battig et al. have reported that duration of lag phase is an important factor in

determining the invasiveness of *S. pneumoniae* infection **[191]**. The authors suggested that based on *in vitro* study, the lag phase duration is correlated positively with the invasiveness of *S. pneumoniae* and negatively with colonization prevalence **[191]**. This suggests that the growth rate and its transition into exponential phase is important factor for virulence of *S. pneumoniae.* Since the bacterial infection conducted in this current study is done in exponential phase of the growth, this aspect of virulence is not captured.

Lag phase offers distinct characteristics compared to the exponential phase. While it is presented in the earliest stage of bacterial growth, it is most poorly studied. Recent study elucidated that the main function of lag phase is to prepare bacteria for exponential growth. A study conducted by Rolfe et al. has focused on gene expression as well as concentration of transient metals in lag phase of *Salmnella enterica* **[192]**. It was presented that in lag phase, there was significant upregulation of genes implicated in metal transport and storage, as well as significant downregulation of metabolic genes. When transient metal concentration was measured with ICP-MS, accumulation of iron, calcium and manganese were observed **[192]**.

Above studies signifies the importance of lag phase in understanding virulence of *S. pneumoniae* in response to Cu NPs exposure. As *S. pneumoniae* is included in human commensal pulmonary flora, the likelihood of interaction between colonized *S. pneumoniae* and Cu NPs occurring in lag phase is higher than in exponential phase. Therefore, when studying the effect of Cu NPs on *S. pneumoniae* infection, conducting study with bacteria in lag phase can provide meaningful insight into Cu NPs exposure.

4.5.6. Evaluation of toxicity for other metal NPs

Though not directly related to the effect of Cu NPs on *S. pneumoniae* infection, conducting experiment on toxicity of other metals that are at high risk for occupational exposure can be valuable. Indium (In) has recently been brought to the attention in the nanotoxicology field. In plays an essential role in production of liquid crystal displays and other electronic devices and been developed in wide range of shapes in nanoscale. They have originally been considered to possess little toxicity due to their insolubility. However, a recent *in vivo* study by Jeong et al. proposed that exposure to In NPs led to prolonged toxicity that lasted longer than other soluble NPs such as Cu and Zn NPs. The authors stated that due to the insolubility, the inhaled NPs are not cleared from alveolar region of lungs and phagocytosed NPs induce continuous inflammatory response leading to further damage **[193]**. Since the use of In is increasing with potential applications in production of electronics, understanding the potential toxicity of In exposure is crucial for the safety of the workers and general public.

In conjunction with an *in vivo* study, conducting the ALI exposure with In would potentially provide mechanistic insight into the toxicity by In NPs. To my knowledge, few studies were conducted with *in vitro* ALI exposure system to evaluate the toxicity of In NPs, suggesting the potential value of this project.

BIBLIOGRAPHY

1. Boholm M, Arvidsson R. A Definition Framework for the Terms Nanomaterial and Nanoparticle. *NanoEthics* 2016, **10**(1)**:** 25-40.

2. Joachim C. To be nano or not to be nano? *Nature Materials* 2005, **4**(2)**:** 107-109.

3. Bowman DM, Hodge GA. A Big Regulatory Tool-Box for a Small Technology. *NanoEthics* 2008, **2**(2)**:** 193-207.

4. Barnard AS. Nanohazards: Knowledge is our first defence. *Nature Materials* 2006, **5**(4)**:** 245-248.

5. Gwinn MR, Vallyathan V. Nanoparticles: health effects--pros and cons. *Environmental health perspectives* 2006, **114**(12)**:** 1818.

6. Pidgeon N, Porritt J, Ryan J, Seaton A, Tendler S, Welland M*, et al.* Nanoscience and nanotechnologies: opportunities and uncertainties. *The Royal Society, The Royal Academy of Engineering* 2004, **29**(07)**:** 2004.

7. Tringides MC, Jałochowski M, Bauer E. Quantum size effects in metallic nanostructures. *Physics Today* 2007, **60**(4)**:** 50-54.

8. Liu J, Lu Y. Accelerated Color Change of Gold Nanoparticles Assembled by DNAzymes for Simple and Fast Colorimetric Pb2+ Detection. *Journal of the American Chemical Society* 2004, **126**(39)**:** 12298-12305.

9. Kahru A, Savolainen K. Potential hazard of nanoparticles: From properties to biological and environmental effects. *Toxicology* 2010, **269**(2)**:** 89-91.

10. Demming A, Österbacka PR, Han DJ-W. Nanotechnology in paper electronics. *Nanotechnology* 2014, **25**(9)**:** 090201.

11. Ahopelto J, Ardila G, Baldi L, Balestra F, Belot D, Fagas G*, et al.* NanoElectronics roadmap for Europe: From nanodevices and innovative materials to system integration. *Solid-State Electronics* 2019, **155:** 7-19.

12. Langer R, Weissleder R. Nanotechnology. *JAMA* 2015, **313**(2)**:** 135-136.

13. Harifi T, Montazer M. Application of nanotechnology in sports clothing and flooring for enhanced sport activities, performance, efficiency and comfort: a review. *Journal of Industrial Textiles* 2017, **46**(5)**:** 1147-1169.

14. Katz LM, Dewan K, Bronaugh RL. Nanotechnology in cosmetics. *Food and Chemical Toxicology* 2015, **85:** 127-137.

15. Baldissera MD, Souza CF, Zeppenfeld CC, Velho MC, Klein B, Abbad LB*, et al.* Dietary supplementation with nerolidol nanospheres improves growth, antioxidant status and fillet fatty acid profiles in Nile tilapia: Benefits of nanotechnology for fish health and meat quality. *Aquaculture* 2020, **516:** 734635.

16. Report HM. Global Nanotechnology Market (by Component and Applications), Funding & Investment, Patent Analysis and 27 Companies Profile & Recent Developments - Forecast to 2024. Report; 2018.

17. Jeevanandam J, Barhoum A, Chan YS, Dufresne A, Danquah MK. Review on nanoparticles and nanostructured materials: history, sources, toxicity and regulations. *Beilstein J Nanotechnol* 2018, **9:** 1050-1074.

18. Warheit DB. Hazard and risk assessment strategies for nanoparticle exposures: how far have we come in the past 10 years? *F1000Research* 2018, **7:** 376-376.

19. Zhang Y, Leu Y-R, Aitken RJ, Riediker M. Inventory of Engineered Nanoparticle-Containing Consumer Products Available in the Singapore Retail Market and Likelihood of Release into the Aquatic Environment. *International Journal of Environmental Research and Public Health* 2015, **12**(8)**:** 8717-8743.

20. Golokhvast KS, Shvedova AA. Galvanic Manufacturing in the Cities of Russia: Potential Source of Ambient Nanoparticles. *PLoS One* 2014, **9**(10).

21. Schulte P, Geraci C, Zumwalde R, Hoover M, Kuempel E. Occupational Risk Management of Engineered Nanoparticles. *Journal of Occupational and Environmental Hygiene* 2008, **5**(4)**:** 239-249.

22. Li R, Wang JJ, Zhou B, Awasthi MK, Ali A, Zhang Z*, et al.* Recovery of phosphate from aqueous solution by magnesium oxide decorated magnetic biochar and its potential as phosphate-based fertilizer substitute. *Bioresource Technology* 2016, **215:** 209-214.

23. Liu J, Jiang J, Meng Y, Aihemaiti A, Xu Y, Xiang H*, et al.* Preparation, environmental application and prospect of biochar-supported metal nanoparticles: A review. *Journal of Hazardous Materials* 2020, **388:** 122026.

24. Tourinho PS, Van Gestel CAM, Lofts S, Svendsen C, Soares AMVM, Loureiro S. Metal-based nanoparticles in soil: Fate, behavior, and effects on soil invertebrates. Hoboken, USA; 2012. pp. 1679-1692.

25. Donaldson K, Stone V, Seaton A, MacNee W. Ambient Particle Inhalation and the Cardiovascular System: Potential Mechanisms. *Environmental Health Perspectives Supplements* 2001, **109:** 523.

26. Wihersaari H, Pirjola L, Karjalainen P, Saukko E, Kuuluvainen H, Kulmala K*, et al.* Particulate emissions of a modern diesel passenger car under laboratory and real-world transient driving conditions. *Environmental Pollution* 2020, **265:** 114948.

27. Maynard RL, Waller RE. Suspended particulate matter and health: new light on an old problem. *Thorax* 1996, **51**(12)**:** 1174-1176.

28. Fushimi A, Kondo Y, Kobayashi S, Fujitani Y, Saitoh K, Takami A*, et al.* Chemical composition and source of fine and nanoparticles from recent direct injection gasoline passenger cars: Effects of fuel and ambient temperature. *Atmospheric Environment* 2016, **124:** 77-84.

29. Yin Y, Tan Z, Hu L, Yu S, Liu J, Jiang G. Isotope Tracers To Study the Environmental Fate and Bioaccumulation of Metal-Containing Engineered Nanoparticles: Techniques and Applications. *Chemical reviews* 2017, **117**(5)**:** 4462-4487.

30. Silkoff PE, Zhang L, Dutton S, Langmack EL, Vedal S, Murphy J*, et al.* Winter air pollution and disease parameters in advanced chronic obstructive pulmonary disease panels residing in Denver, Colorado. *The Journal of Allergy and Clinical Immunology* 2005, **115**(2)**:** 337-344.

31. Meldrum K, Guo C, Marczylo EL, Gant TW, Smith R, Leonard MO. Mechanistic insight into the impact of nanomaterials on asthma and allergic airway disease. *Particle and Fibre Toxicology* 2017, **14**.

32. Roach KA, Anderson SE, Stefaniak AB, Shane HL, Kodali V, Kashon M*, et al.* Surface area- and mass-based comparison of fine and ultrafine nickel oxide lung toxicity and augmentation of allergic response in an ovalbumin asthma model. *Inhalation Toxicology* 2019, **31**(8)**:** 299-324.

33. Armstead AL, Li B. Nanotoxicity: emerging concerns regarding nanomaterial safety and occupational hard metal (WC-Co) nanoparticle exposure. *International Journal of Nanomedicine* 2016, **11:** 6421-6433.

34. Tsai C-J, Huang C-Y, Chen S-C, Ho C-E, Huang C-H, Chen C-W*, et al.* Exposure assessment of nano-sized and respirable particles at different workplaces. *Journal of Nanoparticle Research* 2011, **13**(9)**:** 4161-4172.

35. Viitanen A-K, Uuksulainen S, Koivisto AJ, Hämeri K, Kauppinen T. Workplace Measurements of Ultrafine Particles—A Literature Review. *Annals of Work Exposures and Health* 2017, **61**(7)**:** 749-758.

36. Park JY, Ramachandran G, Raynor PC, Olson GM. Determination of Particle Concentration Rankings by Spatial Mapping of Particle Surface Area, Number, and Mass Concentrations in a Restaurant and a Die Casting Plant. *Journal of Occupational and Environmental Hygiene* 2010, **7**(8)**:** 466-476.

37. Brouwer D, van Duuren-Stuurman B, Berges M, Jankowska E, Bard D, Mark D. From workplace air measurement results toward estimates of exposure? Development of a strategy to assess exposure to manufactured nano-objects. *Journal of Nanoparticle Research* 2009, **11**(8)**:** 1867.

38. Chen BT, Schwegler-Berry D, Cumpston A, Cumpston J, Friend S, Stone S*, et al.* Performance of a scanning mobility particle sizer in measuring diverse types of airborne nanoparticles: Multi-walled carbon nanotubes, welding fumes, and titanium dioxide spray. *Journal of Occupational and Environmental Hygiene* 2016, **13**(7)**:** 501-518.

39. Chen BT, Schwegler-Berry D, McKinney W, Stone S, Cumpston JL, Friend S*, et al.* Multi-walled carbon nanotubes: sampling criteria and aerosol characterization. *Inhalation Toxicology* 2012, **24**(12)**:** 798-820.

40. KENDALL M, HOLGATE S. Health impact and toxicological effects of nanomaterials in the lung. *Respirology* 2012, **17**(5)**:** 743-758.

41. Linnainmaa M, Kangas J, Kalliokoski P. Exposure to Airborne Metals in the Manufacture and Maintenance of Hard Metal and Stellite Blades. *American Industrial Hygiene Association Journal* 1996, **57**(2)**:** 196-201.

42. Liou S-H, Tsai CSJ, Pelclova D, Schubauer-Berigan MK, Schulte PA. Assessing the first wave of epidemiological studies of nanomaterial workers. *J Nanopart Res* 2015, **17:** 413-413.

43. Cobalt in hard metals and cobalt sulfate, gallium arsenide, indium phosphide and vanadium pentoxide. *IARC monographs on the evaluation of carcinogenic risks to humans* 2006, **86:** 1.

44. Moche H, Chevalier D, Vezin H, Claude N, Lorge E, Nesslany F. Genotoxicity of tungsten carbide–cobalt (WC–Co) nanoparticles in vitro: Mechanisms-of-action studies. *Mutation Research/Genetic Toxicology and Environmental Mutagenesis* 2015, **779:** 15-22.

45. Moche H, Chevalier D, Barois N, Lorge E, Claude N, Nesslany F. Tungsten Carbide-Cobalt as a Nanoparticulate Reference Positive Control in In Vitro Genotoxicity Assays. *Toxicological Sciences* 2013, **137**(1)**:** 125-134.

46. Cox A, Venkatachalam P, Sahi S, Sharma N. Silver and titanium dioxide nanoparticle toxicity in plants: A review of current research. *Plant Physiology and Biochemistry* 2016, **107:** 147-163.

47. Wallis LK, Diamond SA, Ma H, Hoff DJ, Al-Abed SR, Li S. Chronic TiO2 nanoparticle exposure to a benthic organism, Hyalella azteca: impact of solar UV radiation and material surface coatings on toxicity. *Science of The Total Environment* 2014, **499:** 356-362.

48. Liu R, Yin L, Pu Y, Liang G, Zhang J, Su Y*, et al.* Pulmonary toxicity induced by three forms of titanium dioxide nanoparticles via intra-tracheal instillation in rats. *Progress in Natural Science* 2009, **19**(5)**:** 573-579.

49. Laomettachit T, Puri IK, Liangruksa M. A two-step model of TiO2 nanoparticle toxicity in human liver tissue. *Toxicology and Applied Pharmacology* 2017, **334:** 47-54.

50. Simeonova PP, Erdely A. Engineered nanoparticle respiratory exposure and potential risks for cardiovascular toxicity: Predictive tests and biomarkers. *Inhalation Toxicology* 2009, **21**(sup1)**:** 68-73.

51. Izquierdo JL, Martínez A, Guzmán E, de Lucas P, Rodríguez JM. Lack of association of ischemic heart disease with COPD when taking into account classical cardiovascular risk factors. *Int J Chron Obstruct Pulmon Dis* 2010, **5:** 387-394.

52. Zhang S, Li J, Lykotrafitis G, Bao G, Suresh S. Size-dependent endocytosis of nanoparticles. *Advanced materials* 2009, **21**(4)**:** 419-424.

53. Zhang Z, Chau PYK, Lai HK, Wong CM. A review of effects of particulate matter-associated nickel and vanadium species on cardiovascular and respiratory systems. *International Journal of Environmental Health Research* 2009, **19**(3)**:** 175-185.

54. Salari Z, Ameri A, Forootanfar H, Adeli-Sardou M, Jafari M, Mehrabani M*, et al.* Microwave-assisted biosynthesis of zinc nanoparticles and their cytotoxic and antioxidant activity. *Journal of Trace Elements in Medicine and Biology* 2017, **39:** 116-123.

55. Mahajan BK, Yu X, Shou W, Pan H, Huang X. Mechanically Milled Irregular Zinc Nanoparticles for Printable Bioresorbable Electronics. *Small* 2017, **13**(17)**:** 1700065.

56. Wallenborn JG, Evansky P, Shannahan JH, Vallanat B, Ledbetter AD, Schladweiler MC*, et al.* Subchronic inhalation of zinc sulfate induces cardiac changes in healthy rats. *Toxicology and Applied Pharmacology* 2008, **232**(1)**:** 69-77.

57. Chuang H-C, Juan H-T, Chang C-N, Yan Y-H, Yuan T-H, Wang J-S*, et al.* Cardiopulmonary toxicity of pulmonary exposure to occupationally relevant zinc oxide nanoparticles. *Nanotoxicology* 2014, **8**(6)**:** 593-604.

58. Chuang K-J, Lee K-Y, Pan C-H, Lai C-H, Lin L-Y, Ho S-C*, et al.* Effects of zinc oxide nanoparticles on human coronary artery endothelial cells. *Food and Chemical Toxicology* 2016, **93:** 138-144.

59. Bezemer G. Particle deposition and clearance from the respiratory tract. 2009.

60. Usmani OS, Biddiscombe MF, Barnes PJ. Regional Lung Deposition and Bronchodilator Response as a Function of [beta]^sub 2^-Agonist Particle Size. *American Journal of Respiratory and Critical Care Medicine* 2005, **172**(12)**:** 1497-1504.

61. Darquenne C. Aerosol deposition in health and disease. *J Aerosol Med Pulm Drug Deliv* 2012, **25**(3)**:** 140-147.

62. Soares T, Ribeiro D, Proença C, Chisté RC, Fernandes E, Freitas M. Size-dependent cytotoxicity of silver nanoparticles in human neutrophils assessed by multiple analytical approaches. *Life Sciences* 2016, **145:** 247-254.

63. Park Y-H, Bae H, Jang Y, Jeong S, Lee H, Ryu W-I*, et al.* Effect of the size and surface charge of silica nanoparticles on cutaneous toxicity. *Molecular & Cellular Toxicology* 2013, **9**(1)**:** 67-74.

64. Forest V, Leclerc L, Hochepied J-F, Trouvé A, Sarry G, Pourchez J. Impact of cerium oxide nanoparticles shape on their in vitro cellular toxicity. *Toxicology in Vitro* 2017, **38:** 136-141.

65. Gorka DE, Osterberg JS, Gwin CA, Colman BP, Meyer JN, Bernhardt ES*, et al.* Reducing Environmental Toxicity of Silver Nanoparticles through Shape Control. *Environmental Science & Technology* 2015, **49**(16)**:** 10093-10098.

66. Mirshafiee V, Kim R, Park S, Mahmoudi M, Kraft ML. Impact of protein pre-coating on the protein corona composition and nanoparticle cellular uptake. *Biomaterials* 2016, **75:** 295-304.

67. Yoshida T, Yoshioka Y, Morishita Y, Aoyama M, Tochigi S, Hirai T*, et al.* Protein corona changes mediated by surface modification of amorphous silica nanoparticles suppress acute toxicity and activation of intrinsic coagulation cascade in mice. *Nanotechnology* 2015, **26**(24)**:** 245101.

68. Oberdörster G. Safety assessment for nanotechnology and nanomedicine: concepts of nanotoxicology. *Journal of Internal Medicine* 2010, **267**(1)**:** 89-105.

69. Docter D, Bantz C, Westmeier D, Galla HJ, Wang Q, Kirkpatrick JC*, et al.* The protein corona protects against size- and dose-dependent toxicity of amorphous silica nanoparticles. *Beilstein J Nanotechnol* 2014, **5:** 1380-1392.

70. Mishra V, Baranwal V, Mishra RK, Sharma S, Paul B, Pandey AC. Titanium dioxide nanoparticles augment allergic airway inflammation and Socs3 expression via NF-κB pathway in murine model of asthma. *Biomaterials* 2016, **92:** 90-102.

71. Park MVDZ, Neigh AM, Vermeulen JP, de La Fonteyne LJJ, Verharen HW, Briedé JJ*, et al.* The effect of particle size on the cytotoxicity, inflammation, developmental toxicity and genotoxicity of silver nanoparticles. *Biomaterials* 2011, **32**(36)**:** 9810-9817.

72. Sun J, Wang S, Zhao D, Hun F, Weng L, Liu H. Cytotoxicity, permeability, and inflammation of metal oxide nanoparticles in human cardiac microvascular endothelial cells. *An International Journal Devoted to Research at the Cellular Level* 2011, **27**(5)**:** 333-342.

73. Capasso L, Camatini M, Gualtieri M. Nickel oxide nanoparticles induce inflammation and genotoxic effect in lung epithelial cells. *Toxicology Letters* 2014, **226**(1)**:** 28-34.

74. Ursula W. Inflammation. *Nature* 2008, **454**(7203)**:** 427.

75. Porcelli EG. Chronic inflammation. *The Journal of the American Dental Association* 2018, **149**(9)**:** 750-751.

76. Halliwell B. Reactive oxygen species in living systems: Source, biochemistry, and role in human disease. *The American Journal of Medicine* 1991, **91**(3)**:** S14-S22.

77. MacDowell KS, Marsá MD, Buenache E, Villatoro JML, Moreno B, Leza JC*, et al.* Inflammatory and antioxidant pathway dysfunction in borderline personality disorder. *Psychiatry Research* 2020, **284:** 112782.

78. Lushchak VI. Free radicals, reactive oxygen species, oxidative stress and its classification. *Chemico-Biological Interactions* 2014, **224:** 164-175.

79. Savolainen K, Alenius H, Norppa H, Pylkkänen L, Tuomi T, Kasper G. Risk assessment of engineered nanomaterials and nanotechnologies—A review. *Toxicology* 2010, **269**(2)**:** 92-104.

80. Manke A, Wang L, Rojanasakul Y. Mechanisms of Nanoparticle-Induced Oxidative Stress and Toxicity. *BioMed Research International* 2013, **2013**.

81. Yang H, Liu C, Yang D, Zhang H, Xi Z. Comparative study of cytotoxicity, oxidative stress and genotoxicity induced by four typical nanomaterials: the role of particle size, shape and composition. *Journal of Applied Toxicology* 2009, **29**(1)**:** 69-78.

82. Knaapen AM, Borm PJA, Albrecht C, Schins RPF. Inhaled particles and lung cancer. Part A: Mechanisms. *International Journal of Cancer* 2004, **109**(6)**:** 799-809.

83. Sun L, Li Y, Liu X, Jin M, Zhang L, Du Z*, et al.* Cytotoxicity and mitochondrial damage caused by silica nanoparticles. *Toxicology in Vitro* 2011, **25**(8)**:** 1619-1629.

84. Semisch A, Ohle J, Witt B, Hartwig A. Cytotoxicity and genotoxicity of nano - and microparticulate copper oxide: role of solubility and intracellular bioavailability. *Particle and Fibre Toxicology* 2014, **11:** 10.

85. Zhao X, Striolo A, Cummings PT. C 60 Binds to and Deforms Nucleotides. *Biophysical Journal* 2005, **89**(6)**:** 3856-3862.

86. Xu Y, Ming-Tzo W, Ou-Yang HD, Walker SG, Hong Zhan W, Gordon CR*, et al.* Exposure to TiO2 nanoparticles increases Staphylococcus aureus infection of HeLa cells. *Journal of Nanobiotechnology* 2016, **14**.

87. Coggon D, Inskip H, Winter P, Pannett B. Lobar pneumonia: an occupational disease in welders. *The Lancet* 1994, **344**(8914)**:** 41-43.

88. Torén K, Qvarfordt I, Bergdahl IA, Järvholm B. Increased mortality from infectious pneumonia after occupational exposure to inorganic dust, metal fumes and chemicals. *Thorax* 2011, **66**(11)**:** 992-996.

89. Torén K, Blanc PD, Naidoo RN, Murgia N, Qvarfordt I, Aspevall O*, et al.* Occupational exposure to dust and to fumes, work as a welder and invasive pneumococcal disease risk. *Occupational and Environmental Medicine* 2020, **77**(2)**:** 57-63.

90. Antonini JM. Health effects of welding. *Critical Reviews in Toxicology* 2003, **33**(1)**:** 61-103.

91. Suri R, Periselneris J, Lanone S, Zeidler-Erdely PC, Melton G, Palmer KT*, et al.* Exposure to welding fumes and lower airway infection with Streptococcus pneumoniae. *The Journal of allergy and clinical immunology* 2016, **137**(2)**:** 527-534.e527.

92. Watt JP, Wolfson LJ, O'Brien KL, Henkle E, Deloria-Knoll M, McCall N*, et al.* Burden of disease caused by Haemophilus influenzae type b in children younger than 5 years: global estimates. *The Lancet* 2009, **374**(9693)**:** 903-911.

93. Novick S, Shagan M, Blau K, Lifshitz S, Givon-Lavi N, Grossman N*, et al.* Adhesion and invasion of Streptococcus pneumoniae to primary and secondary respiratory epithelial cells. *Molecular medicine reports* 2017, **15**(1)**:** 65-74.

94. Marrie TJ. Bacteremic Pneumococcal Pneumonia Mortality Rate: Is It Really Different in Sweden? *Chest* 1993, **103**(3)**:** 658-660.

95. Leu HS, Kaiser DL, Mori M, Woolson RF, Wenzel RP. Hospital-acquired pneumonia. Attributable mortality and morbidity. *American journal of epidemiology* 1989, **129**(6)**:** 1258-1267.

96. Vernatter J, Pirofski L-A. Current concepts in host–microbe interaction leading to pneumococcal pneumonia. *Current Opinion in Infectious Diseases* 2013, **26**(3)**:** 277-283.

97. Bogaert D, de Groot R, Hermans P. Streptococcus pneumoniae colonisation: the key to pneumococcal disease. *The Lancet Infectious Diseases* 2004, **4**(3)**:** 144-154.

98. Ofek I, Edward B, Abraham S. Bacterial adhesion. *The Prokaryotes: Human Microbiology* 2013**:** 107-123.

99. Beachey EH. Bacterial Adherence: Adhesin-Receptor Interactions Mediating the Attachment of Bacteria to Mucosal Surfaces. *The Journal of Infectious Diseases* 1981, **143**(3)**:** 325-345.

100. Krachler AM, Orth K. Targeting the bacteria-host interface: Strategies in anti-adhesion therapy. *Virulence* 2013, **4**(4)**:** 284-294.

101. Ofek I. *Bacterial adhesion to animal cells and tissues*. Washington, D.C. : ASM Press: Washington, D.C., 2003.

102. Mitchell AM, Mitchell TJ. Streptococcus pneumoniae: virulence factors and variation. *Clinical Microbiology and Infection* 2010, **16**(5)**:** 411-418.

103. Sanchez C, Hinojosa C, Shivshankar P, Hyams C, Camberlein E, Brown J*, et al.* Changes in capsular serotype alter the surface exposure of pneumococcal adhesins and impact virulence. *PLoS One* 2011.

104. Hu D-K, Liu Y, Li X-Y, Qu Y. In vitro expression of Streptococcus pneumoniae ply gene in human monocytes and pneumocytes. *European Journal of Medical Research* 2015, **20**(1)**:** 52.

105. Frolet C, Beniazza M, Roux L, Gallet B, Noirclerc-Savoye M, Vernet T*, et al.* New adhesin functions of surface-exposed pneumococcal proteins. *BMC Microbiology* 2010, **10:** 190-190.

106. Dupré DJ, Chen Z, Le Gouill C, Thériault C, Parent J-L, Rola-Pleszczynski M*, et al.* Trafficking, ubiquitination, and down-regulation of the human platelet-activating factor receptor. *The Journal of biological chemistry* 2003, **278**(48)**:** 48228-48235.

107. Diana RC, Norma PG, Craig G, Ilona I-H, Elaine IT. Streptococcus pneumoniae anchor to activated human cells by the receptor for platelet-activating factor. *Nature* 1995, **377**(6548)**:** 435.

108. Grigg J, Walters H, Sohal SS, Wood-Baker R, Reid DW, Xu C-B*, et al.* Cigarette smoke and platelet-activating factor receptor dependent adhesion of Streptococcus pneumoniae to lower airway cells. *Thorax* 2012, **67**(10)**:** 908-913.

109. Mushtaq N, Ezzati M, Hall L, Dickson I, Kirwan M, Png KMY*, et al.* Adhesion of Streptococcus pneumoniae to human airway epithelial cells exposed to urban particulate matter. *The Journal of Allergy and Clinical Immunology* 2011, **127**(5)**:** 1236-1242.e1232.

110. Weinberger DM, Harboe ZB, Sanders EAM, Ndiritu M, Klugman KP, Rückinger S*, et al.* Association of serotype with risk of death due to pneumococcal pneumonia: a meta-analysis. *Clinical infectious diseases : an official publication of the Infectious Diseases Society of America* 2010, **51**(6)**:** 692-699.

111. Heffron R. *Pneumonia, with Special Reference to Pneumococcus Lobar Pneumonia*. Harvard University Press, 1979.

112. Hathaway LJ, Grandgirard D, Valente LG, Täuber MG, Leib SL. Streptococcus pneumoniae capsule determines disease severity in experimental pneumococcal meningitis. *Open Biol* 2016, **6**(3)**:** 150269.

113. Gupta D, Agarwal R, Aggarwal AN, Singh N, Mishra N, Khilnani GC*, et al.* Guidelines for diagnosis and management of community- and hospital-acquired pneumonia in adults: Joint ICS/NCCP(I) recommendations. *Lung India : official organ of Indian Chest Society* 2012, **29**(Suppl 2)**:** S27.

114. Balicer RD, Zarka S, Levine H, Klement E, Sela T, Porat N*, et al.* Control of Streptococcus pneumoniae serotype 5 epidemic of severe pneumonia among young army recruits by mass antibiotic treatment and vaccination. *Vaccine* 2010, **28**(34)**:** 5591-5596.

115. D'angelo R, Gonzales J, Tata A, Heil E, Patel D, Shanholtz C. 751: HEALTHCARE-ASSOCIATED PNEUMONIA TREATMENT CHARACTERIZATION IN MEDICAL ICU PATIENTS. *Critical Care Medicine* 2015, **43**(12 Suppl 1)**:** 189-189.

116. Aguilar L, Gimnez MJ, Garcia-Rey C, Martn JE. New strategies to overcome antimicrobial resistance in Streptococcus pneumoniae with -lactam antibiotics. *Journal of Antimicrobial Chemotherapy* 2002, **50**(3)**:** 93-100.

117. Schroeder MR, Stephens DS. Macrolide Resistance in Streptococcus pneumoniae. *Frontiers in cellular and infection microbiology* 2016, **6:** 98-98.

118. Patel SN, McGeer A, Melano R, Tyrrell GJ, Green K, Pillai DR*, et al.* Susceptibility of Streptococcus pneumoniae to fluoroquinolones in Canada. *Antimicrobial agents and chemotherapy* 2011, **55**(8)**:** 3703-3708.

119. Guervil DJ, Kaye KS, Hassoun A, Cole P, Huang X-Y, Friedland HD. Ceftaroline fosamil as first-line versus second-line treatment for acute bacterial skin and skin structure infections (ABSSSI) or community-acquired bacterial pneumonia (CABP). *Journal of Chemotherapy* 2016, **28**(3)**:** 180-186.

120. Matthew AC, David S. Fix the antibiotics pipeline. *Nature* 2011, **472**(7341)**:** 32.

121. Geno KA, Gilbert GL, Song JY, Skovsted IC, Klugman KP, Jones C*, et al.* Pneumococcal Capsules and Their Types: Past, Present, and Future. *Clinical microbiology reviews* 2015, **28**(3)**:** 871-899.

122. Latifi-Navid H, Latifi-Navid S, Mostafaiy B, Jamalkandi SA, Ahmadi A. Pneumococcal Disease and the Effectiveness of the PPV23 Vaccine in Adults: A Two-Stage Bayesian Meta-Analysis of Observational and RCT Reports. *Scientific reports* 2018, **8**(1)**:** 11051-11051.

123. LeBlanc JJ, ElSherif M, Ye L, MacKinnon-Cameron D, Ambrose A, Hatchette TF*, et al.* Streptococcus pneumoniae serotype 3 is masking PCV13-mediated herd immunity in Canadian adults hospitalized with community acquired pneumonia: A study from the Serious Outcomes Surveillance (SOS) Network of the Canadian immunization research Network (CIRN). *Vaccine* 2019, **37**(36)**:** 5466-5473.

124. Jones RN, Jacobs MR, Sader HS. Evolving trends in Streptococcus pneumoniae resistance: implications for therapy of community-acquired bacterial pneumonia. *International Journal of Antimicrobial Agents* 2010, **36**(3)**:** 197-204.

125. Bryce J, Boschi-Pinto C, Shibuya K, Black RE, et al. WHO estimates of the causes of death in children. *The Lancet* 2005, **365**(9465)**:** 1147-1152.

126. Sheppard CL, Clark J, Slack MPE, Fry NK, Harrison TG. Use of a serotype-specific urine immunoassay to determine the course of a hospital outbreak of Streptococcus pneumoniae complicated by influenza A. *JMM Case Rep* 2016, **3**(1)**:** e005002-e005002.

127. Meehan T, Fine M, Krumholz H, Scinto J. Quality of care, process, and outcomes in elderly patients with pneumonia. *JAMA* 1997, **278**(23)**:** 2080-2084.

128. Gleich S, Morad Y, Echague R, Miller JR, Kornblum J, Sampson JS*, et al.* Streptococcus pneumoniae Serotype 4 Outbreak in a Home for the Aged: Report and Review of Recent Outbreaks. *Infection Control and Hospital Epidemiology* 2000, **21**(11)**:** 711-717.

129. Fry AM, Shay DK, Holman RC, Curns AT, Anderson LJ. Trends in Hospitalizations for Pneumonia Among Persons Aged 65 Years or Older in the United States, 1988-2002. *JAMA* 2005, **294**(21)**:** 2712-2719.

130. Ewing J, Patterson L, Irvine N, Doherty L, Loughrey A, Kidney J*, et al.* Serious pneumococcal disease outbreak in men exposed to metal fume - detection, response and future prevention through pneumococcal vaccination. *Vaccine* 2017, **35**(32)**:** 3945-3950.

131. Suri R, Periselneris J, Lanone S, Zeidler - Erdely P, Melton G, Palmer K*, et al.* Exposure to welding fumes and lower airway infection with Streptococcus pneumoniae. *Journal of Allergy and Clinical Immunology* 2015.

132. Wong A, Marrie TJ, Garg S, Kellner JD, Tyrrell GJ. Welders are at increased risk for invasive pneumococcal disease. *International Journal of Infectious Diseases* 2010, **14**(9)**:** e796-e799.

133. Immunization NACo. Pneumococcal vaccine. Canadian immunization guide. Evergreen ed. Ottawa. *ON: Public Health Agency of Canada (PHAC) Accessed May* 2014, **18**.

134. Beekhuijzen M. The era of 3Rs implementation in developmental and reproductive toxicity (DART) testing: Current overview and future perspectives. *Reproductive Toxicology* 2017, **72:** 86-96.

135. Dhawan A, Sharma V. Toxicity assessment of nanomaterials: methods and challenges. *Analytical and Bioanalytical Chemistry* 2010, **398**(2)**:** 589-605.

136. Sayes C, Reed K, Subramoney S, Abrams L, Warheit D. Can in vitro assays substitute for in vivo studies in assessing the pulmonary hazards of fine and nanoscale materials? *An Interdisciplinary Forum for Nanoscale Science and Technology* 2009, **11**(2)**:** 421-431.

137. Arora S, Rajwade JM, Paknikar KM. Nanotoxicology and in vitro studies: The need of the hour. *Toxicology and Applied Pharmacology* 2012, **258**(2)**:** 151-165.

138. Jones CF, Grainger DW. In vitro assessments of nanomaterial toxicity. *Advanced Drug Delivery Reviews* 2009, **61**(6)**:** 438-456.

139. Jing X, Park JH, Peters TM, Thorne PS. Toxicity of copper oxide nanoparticles in lung epithelial cells exposed at the air–liquid interface compared with in vivo assessment. *Toxicology in Vitro* 2015, **29**(3)**:** 502-511.

140. Farcal L, Fernando Torres A, Luisana Di C, Rotoli BM, Bussolati O, Bergamaschi E*, et al.* Comprehensive In Vitro Toxicity Testing of a Panel of Representative Oxide Nanomaterials: First Steps towards an Intelligent Testing Strategy. *PLoS One* 2015, **10**(5).

141. Adam N, Leroux F, Knapen D, Bals S, Blust R. The uptake and elimination of ZnO and CuO nanoparticles in Daphnia magna under chronic exposure scenarios. *Water Research* 2015, **68:** 249-261.

142. Müller L, Gasser M, Raemy DO, Herzog F, Brandenberger C, Schmid O*, et al.* Realistic exposure methods for investigating the interaction of nanoparticles with the lung at the air-liquid interface in vitro. *Insciences J* 2011, **1**(1)**:** 30-64.

143. Lenz A, Karg E, Lentner B, Dittrich V, Brandenberger C, Rothen-Rutishauser B*, et al.* A dose-controlled system for air-liquid interface cell exposure and application to zinc oxide nanoparticles. *Particle and Fibre Toxicology* 2009, **6**(1)**:** 32.

144. Öhlinger K, Kolesnik T, Meindl C, Gallé B, Absenger-Novak M, Kolb-Lenz D*, et al.* Air-liquid interface culture changes surface properties of A549 cells. *Toxicology in Vitro* 2019, **60:** 369-382.

145. Kim JS, Adamcakova-Dodd A, O'Shaughnessy PT, Grassian VH, Thorne PS. Effects of copper nanoparticle exposure on host defense in a murine pulmonary infection model. *Particle and Fibre Toxicology* 2011, **8**(1).

146. Gulati K, Ray A. CHAPTER 40 - Immunotoxicity. In: Gupta RC (ed). *Handbook of Toxicology of Chemical Warfare Agents*. Academic Press: San Diego, 2009, pp 595-609.

147. Bisgaard H, Ebrary I, O'Callaghan C, Smaldone GC. Drug delivery to the lung. New York: New York : M. Dekker; 2002.

148. Steiner S, Majeed S, Kratzer G, Vuillaume G, Hoeng J, Frentzel S. Characterization of the Vitrocell® 24/48 aerosol exposure system for its use in exposures to liquid aerosols. *Toxicology in Vitro* 2017, **42:** 263-272.

149. Salem H, Katz SA. *Inhalation Toxicology, Third Edition*. Taylor & Francis, 2014.

150. Duan H, Romay FJ, Li C, Naqwi A, Deng W, Liu BYH. Generation of monodisperse aerosols by combining aerodynamic flow-focusing and mechanical perturbation. *Aerosol Science and Technology* 2016, **50**(1)**:** 17-25.

151. Amatngalim GD, Hiemstra PS. Airway Epithelial Cell Function and Respiratory Host Defense in Chronic Obstructive Pulmonary Disease. *Chin Med J (Engl)* 2018, **131**(9)**:** 1099-1107.

152. Bustin SA, Benes V, Garson JA, Hellemans J, Huggett J, Kubista M*, et al.* The MIQE guidelines: minimum information for publication of quantitative real-time PCR experiments. *Clinical chemistry* 2009, **55**(4)**:** 611-622.

153. Shingles R, North M, McCarty RE. Direct Measurement of Ferrous Ion Transport across Membranes Using a Sensitive Fluorometric Assay. *Analytical Biochemistry* 2001, **296**(1)**:** 106-113.

154. Forrer R, Gautschi K, Lutz H. Simultaneous measurement of the trace elements Al, As, B, Be, Cd, Co, Cu, Fe, Li, Mn, Mo, Ni, Rb, Se, Sr, and Zn in human serum and their reference ranges by ICP-MS. *Biological Trace Element Research* 2001, **80**(1)**:** 77-93.

155. Malavolta M, Piacenza F, Basso A, Giacconi R, Costarelli L, Pierpaoli S*, et al.* Speciation of trace elements in human serum by micro anion exchange chromatography coupled with inductively coupled plasma mass spectrometry. *Analytical Biochemistry* 2012, **421**(1)**:** 16-25.

156. Zavala J, Greenan R, Krantz QT, DeMarini DM, Higuchi M, Gilmour MI*, et al.* Regulating temperature and relative humidity in air–liquid interface in vitro systems eliminates cytotoxicity resulting from control air exposures. *Toxicology Research* 2017, **6**(4)**:** 448-459.

157. Gaetke LM, Chow CK. Copper toxicity, oxidative stress, and antioxidant nutrients. *Toxicology* 2003, **189**(1-2)**:** 147-163.

158. Kim JS, Peters TM, O'Shaughnessy PT, Adamcakova-Dodd A, Thorne PS. Validation of an in vitro exposure system for toxicity assessment of air-delivered nanomaterials. *Toxicology in vitro : an international journal published in association with BIBRA* 2013, **27**(1)**:** 164-173.

159. Könczöl M, Goldenberg E, Ebeling S, Schäfer B, Garcia-Käufer M, Gminski R*, et al.* Cellular Uptake and Toxic Effects of Fine and Ultrafine Metal-Sulfate Particles in Human A549 Lung Epithelial Cells. *Chemical Research in Toxicology* 2012, **25**(12)**:** 2687-2703.

160. Srivastava RK, Rahman Q, Kashyap MP, Lohani M, Pant AB. Ameliorative effects of dimetylthiourea and N-acetylcysteine on nanoparticles induced cyto-genotoxicity in human lung cancer cells-A549. *PloS one* 2011, **6**(9)**:** 1.

161. Zou Y, Jin C, Su Y, Li J, Zhu B. Water soluble and insoluble components of urban PM2.5 and their cytotoxic effects on epithelial cells (A549) in vitro. *Environmental Pollution* 2016, **212:** 627-635.

162. Restrepo AV, Salazar BE, Agudelo M, Rodriguez CA, Zuluaga AF, Vesga O. Optimization of culture conditions to obtain maximal growth of penicillin-resistant Streptococcus pneumoniae. *BMC microbiology* 2005, **5:** 34-34.

163. Tarpay MM, Welch DF, Marks MI. Antimicrobial susceptibility testing of Streptococcus pneumoniae by micro-broth dilution. *Antimicrobial Agents and Chemotherapy* 1980, **18**(4)**:** 579-581.

164. Henriques-Normark B, Tuomanen EI. The pneumococcus: epidemiology, microbiology, and pathogenesis. *Cold Spring Harb Perspect Med* 2013, **3**(7)**:** a010215.

165. Turula H, Wobus C. The Role of the Polymeric Immunoglobulin Receptor and Secretory Immunoglobulins during Mucosal Infection and Immunity. *Viruses* 2018, **10**(5)**:** 237.

166. Anderton JM, Rajam G, Romero-Steiner S, Summer S, Kowalczyk AP, Carlone GM*, et al.* E-cadherin is a receptor for the common protein pneumococcal surface adhesin A (PsaA) of Streptococcus pneumoniae. *Microbial Pathogenesis* 2007, **42**(5-6)**:** 225-236.

167. Iovino F, Brouwer MC, Beek D, Molema G, Bijlsma JJE. Signalling or binding: the role of the platelet-activating factor receptor in invasive pneumococcal disease. 2013. pp. 870-881.

168. Asano M, Komiyama K. Polymeric immunoglobulin receptor. *Journal of oral science* 2011, **53**(2)**:** 147-156.

169. Elm C, Braathen R, Bergmann S, Frank R, Vaerman J-P, Kaetzel CS*, et al.* Ectodomains 3 and 4 of human polymeric Immunoglobulin receptor (hpIgR) mediate invasion of Streptococcus pneumoniae into the epithelium. *The Journal of biological chemistry* 2004, **279**(8)**:** 6296-6304.

170. Smyth D, Leung G, Fernando M, McKay DM. Reduced Surface Expression of Epithelial E-Cadherin Evoked by Interferon-Gamma Is Fyn Kinase-Dependent. *PLoS One* 2012, **7**(6).

171. Zhang J-R, Mostov KE, Lamm ME, Nanno M, Shimida S-I, Ohwaki M*, et al.* The Polymeric Immunoglobulin Receptor Translocates Pneumococci across Human Nasopharyngeal Epithelial Cells. *Cell* 2000, **102**(6)**:** 827-837.

172. Yang HH, Pang JH, Hung RY, Chau LY. Transcriptional regulation of platelet-activating factor receptor gene in B lymphoblastoid Ramos cells by TGF-beta. *Journal of immunology (Baltimore, Md : 1950)* 1997, **158**(6)**:** 2771-2778.

173. Dagenais P, Thivierge M, Parent JL, Stankova J, Rola-Pleszczynski M. Augmented expression of platelet-activating factor receptor gene by TNF- alpha through transcriptional activation in human monocytes. *Journal of Leukocyte Biology* 1997, **61**(1)**:** 106-112.

174. Ouellet S, Müller E, Rola-Pleszczynski M. IFN-gamma up-regulates platelet-activating factor receptor gene expression in human monocytes. *Journal of immunology (Baltimore, Md : 1950)* 1994, **152**(10)**:** 5092-5099.

175. Nishioka C, Ikezoe T, Pan B, Xu K, Yokoyama A. MicroRNA-9 plays a role in interleukin-10-mediated expression of E-cadherin in acute myelogenous leukemia cells. *Cancer Science* 2017, **108**(4)**:** 685-695.

176. Moreno J, Mikhailenko I, Tondravi M, Keegan A. IL-4 promotes the formation of multinucleated giant cells from macrophage precursors by a STAT6-dependent, homotypic mechanism: Contribution of E-cadherin. *Journal of leukocyte biology* 2008, **82:** 1542-1553.

177. Cassee FR, Kreyling W, Aitken R, Poland C. Dosimetry and Toxicology of Nanosized Particles and Fibres. In: Viana M (ed). *Indoor and Outdoor Nanoparticles: Determinants of Release and Exposure Scenarios*. Springer International Publishing: Cham, 2016, pp 1-18.

178. Jeanson S, Floury J, Gagnaire V, Lortal S, Thierry A. Bacterial Colonies in Solid Media and Foods: A Review on Their Growth and Interactions with the Micro-Environment. *Frontiers in Microbiology* 2015, **6**(1284).

179. Hurbánková M, Hrašková D, Marcišiaková J, Kysucká K, Moricová Š. Nanoparticles from welding and their effects on health. *Pracovni Lekarstvi* 2015, **67:** 12-17.

180. Pećina-Slaus N. Tumor suppressor gene E-cadherin and its role in normal and malignant cells. *Cancer Cell Int* 2003, **3**(1)**:** 17-17.

181. Ko J-W, Park J-W, Shin N-R, Kim J-H, Cho Y-K, Shin D-H*, et al.* Copper oxide nanoparticle induces inflammatory response and mucus production via MAPK signaling in human bronchial epithelial cells. *Environmental Toxicology and Pharmacology* 2016, **43:** 21-26.

182. Sanjabi S, Zenewicz LA, Kamanaka M, Flavell RA. Anti-inflammatory and pro-inflammatory roles of TGF-beta, IL-10, and IL-22 in immunity and autoimmunity. *Curr Opin Pharmacol* 2009, **9**(4)**:** 447-453.

183. Han Z, Kang D, Joo Y, Lee J, Oh G-H, Choi S*, et al.* TGF-β downregulation-induced cancer cell death is finely regulated by the SAPK signaling cascade. *Exp Mol Med* 2018, **50**(12)**:** 1-19.

184. Xu C-C, Wu L-M, Sun W, Zhang N, Chen W-S, Fu X-N. Effects of TGF-β signaling blockade on human A549 lung adenocarcinoma cell lines. *Mol Med Rep* 2011, **4**(5)**:** 1007-1015.

185. Jeng HA, Swanson J. Toxicity of Metal Oxide Nanoparticles in Mammalian Cells. *Journal of Environmental Science and Health, Part A* 2006, **41**(12)**:** 2699-2711.

186. Devaux CA, Mezouar S, Mege J-L. The E-Cadherin Cleavage Associated to Pathogenic Bacteria Infections Can Favor Bacterial Invasion and Transmigration, Dysregulation of the Immune Response and Cancer Induction in Humans. *Frontiers in microbiology* 2019, **10:** 2598-2598.

187. Johnston JW, Myers LE, Ochs MM, Benjamin WH, Briles DE, Hollingshead SK. Lipoprotein PsaA in virulence of Streptococcus pneumoniae: surface accessibility and role in protection from superoxide. *Infection and immunity* 2004, **72**(10)**:** 5858-5867.

188. De Wals P. Commentary on paradoxical observations pertaining to the impact of the 13-valent pneumococcal conjugate vaccine on serotype 3 Streptococcus pneumoniae infections in children. *Vaccine* 2018, **36**(37)**:** 5495-5496.

189. Johnson MDL, Kehl-Fie TE, Klein R, Kelly J, Burnham C, Mann B*, et al.* Role of copper efflux in pneumococcal pathogenesis and resistance to macrophage-mediated immune clearance. *Infection and immunity* 2015, **83**(4)**:** 1684-1694.

190. Ladomersky E, Petris MJ. Copper tolerance and virulence in bacteria. *Metallomics* 2015, **7**(6)**:** 957-964.

191. Bättig P, Hathaway LJ, Hofer S, Mühlemann K. Serotype-specific invasiveness and colonization prevalence in Streptococcus pneumoniae correlate with the lag phase during in vitro growth. *Microbes and Infection* 2006, **8**(11)**:** 2612-2617.

192. Rolfe MD, Rice CJ, Lucchini S, Pin C, Thompson A, Cameron ADS*, et al.* Lag phase is a distinct growth phase that prepares bacteria for exponential growth and involves transient metal accumulation. *J Bacteriol* 2012, **194**(3)**:** 686-701.

193. Jeong J, Kim J, Seok S, Cho W-S. Indium oxide (In 2 O 3) nanoparticles induce progressive lung injury distinct from lung injuries by copper oxide (CuO) and nickel oxide (NiO) nanoparticles. *Archives of Toxicology* 2016, **90**(4)**:** 817-828.